An efficient way of visualization of mutual solubility data in the whole range of compositions[1]

Vladimir Diky

Applied Chemicals and Materials Division, National Institute of Standards and Technology, Boulder, Colorado 80305-3337, USA

*Corresponding author. Tel.: +1-303-497-4124. E-mail address: vladimir.diky@nist.gov (V. Diky).

ABSTRACT: An efficient way or stretching phase diagrams is proposed that represents the whole composition range and reveals details of low-solubility regions. It is based on the transformation of mole fraction x_1 to $\log_{10}(x_1/x_2) = \log_{10}(x_1/(1 - x_1))$ for binary mixtures. While the primary application is liquid-liquid and solid-liquid equilibria, the use of this method for other properties may also be beneficial. An extension on ternary mixtures is also discussed.

---

1. Introduction

Though mathematical analysis of physico-chemical data is very advanced these days, graphical representation is probably the most efficient way to communicate such information to a human. Traditionally, binary phase equilibria are shown on rectangular plots in coordinates $x_1 - T$ (*e.g.*, Fig. 1 of a recent Solubility Data Series publication;[1] a similar plot generated by NIST ThermoData Engine (TDE) software[2] for 3 selected literature sources is shown in Figure 1a) and ternary equilibria on triangular plots in coordinates $x_1 - x_2$ (*e.g.*, Fig. 1 in Góral et al.;[6] a similar plot generated by TDE software is shown in Figure 2). Binary vapor-liquid equilibria may be represented in $x_1 - p$ coordinates (isothermal data sets) or $x_1 - y_1$ (compositions of coexisting phases) where the ordinate may represent volatility ratio or a so-called K-value instead of plain y_1. A common challenge in representing low mutual solubility data is caused by the fact that the data points lie very closely to the $x_1 = 0$ or $x_1 = 1$ lines or to the triangle facets in a linear scale (Figures 1a and 2), and even large relative deviations are invisible. The use of a logarithmic scale allows one to better represent one minor component while the other side of the plot is still collapsed to a line (Figure 1b). Sometimes researches combine magnified or logarithmic representations of two opposite low-concentration regions for binary mixtures (*e.g.*, Fig. 1 in Possani et al.[9]), but it is a combination of two lines in different coordinates (x_1 and x_2), which is not continuous, and cannot show the whole picture. Hand[10] and Othmer and Tobias[11] used content ratios for representation of ternary systems that is efficient for magnification of spots but cannot be used for representation of whole diagrams. To summarize, there was no way to represent the whole phase diagram known to the author at the beginning of this research capable to simultaneously reveal details in all composition areas. This paper proposes a solution for binary mixtures and data transformations that can be useful for ternary mixtures.

2. Binary mixtures

The proposed method for binary mixtures (Figure 1c), called here composition-stretched representation, consists of the use of the decimal logarithm of mole-fraction ratio $\log_{10}(x_1/x_2) = \log_{10}(x_1/(1 - x_1))$ vs. temperature. That function changes from minus infinity to plus infinity when x_1 changes from 0 to 1, equally representing relative changes in composition and revealing trends, consistency of the data, and deviations from models in the whole composition range. It allows a human to visually reveal trends and inconsistencies in the complete data set from a single plot. The composition-stretched representation is close to the logarithmic view in terms of x_1 and x_2 in the regions of small x_1 and x_2, respectively, and close to the linear scale in the middle. Several examples involve both low solubility and high solubility regions. Figure 1c reveals inconsistency of the solubility data at low x_1 invisible in the linear scale. As shown in Figure 3, a revealed feature is a surprising symmetry of the LLE plot in the transformed coordinates. A smooth transition eliminates the distinction between regions revealing inconsistencies in a relative scale (Figure 4).

The closest way of representation used by other authors is that used in Fig. 1 in Possani et al.[9] A common feature with the proposed method is that the numerical values of the transformed composition variable: $\log_{10}(x_1)$ and $\log_{10}(x_2)$ at low and high x_1 in Possani et al.[9] represent the asymptotic behavior of the function at $\log_{10}(x_1/x_2)$ at $x_1 \to 0$ and $x_1 \to 1$, respectively. The following two features are in favor of the proposed method. (1) The same transformation is used in the whole composition range and, hence, the same quantity is used as abscissa while the plot in Possani et al.[9] is an overlay of two plots. (2) The proposed transformation can represent data

in the whole range of concentration in a relative scale, including two dilute-solution regions and the middle region.

While the primary purpose of this development is liquid-liquid (LLE) and solid-liquid (SLE) equilibria, it can be also applied to vapor-liquid equilibria (VLE) and even other properties (Figure 5) for revealing low-concentration behavior and assessing the consistency between low-concentration and high-concentration data. Composition-stretched plots can also show model curves (Figure 6c). That example (benzene + water) strongly supports the advantages of the composition-stretched representation over the linear (Figure 6a) and logarithmic (Figure 6b) representations. Figure 6c also reveals temperature dependence of the solubility of benzene in water that is impossible in the linear scale (Figure 6a). In contrast to the logarithmic representation of experimental and calculated data in Fig. 2-3 in Possani et al.[9] where they belong to different axes, the composition-stretched representation uses thecomposition variable once and allows an additional state variable (e.g., temperature) in a plot. Application of the composition-stretched representation to a combination of LLE and SLE data (Figure 7b) magnifies the areas surrounding monotectic points for any low mutual solubility that are impossible to analyze in the linear scale (Figure 7a).

Composition-stretched plots are also convenient for representation of uncertainties (Figure 8) and their relation to data scatter. Large uncertainties of solubility values that are expected to be asymmetrical in terms of mole or mass fraction become symmetrical in terms of $\log_{10}(x_1/x_2)$. For example, an error by a factor of 5 would be from $-0.8x_1$ to $5x_1$ in the linear scale and approximately $\pm\log_{10}(5)$ in $\log_{10}(x_1/x_2)$ scale. The uncertainty 0.0001 in mole fraction claimed by Grozdanic et al.[5] converted to the $\log_{10}(x_1/x_2)$ scale U(plot scale) = $\log_{10}(1 + U(x_1)/x_1)$ is represented in Figure 8 by horizontal bars. As large uncertainties and curve deviations are

common for low solubility measurements, the function $\log_{10}(x_1/x_2)$ can also be used for assigning weights before model fitting, revealing outliers, and calculating covariance matrices. That can be implemented through fitting $\log_{10}(x_1/x_2)$ instead of fitting x_1 directly.

3. Ternary mixtures

Similar representation of LLE and SLE for ternary mixtures can be built if fractions of all components are stretched along different axes (where one variable would be dependent on the other two). That would need a third dimension and is not practical. Two-dimensional representations are less universal and require some creativity, but they can still be valuable. Two variants are proposed here. One is a three-way stretching when the composition (mole or mass fractions) is transformed to Cartesian plot coordinates in 3 steps. First, a triangle is built:

$$X_t = x_1+0.5\cdot x_2;\ Y_t = (3^{0.5}/2)\cdot x_2. \quad (1)$$

Then the triangle is centered:

$$X_c = X_t - 0.5;\ Y_c = Y_t - 3^{0.5}/6 \quad (2)$$

Finally, each data point is translated away from the midpoint of the triangle on the basis of the content of the minor component i (the component with the smallest mole fraction, or mass fraction if the plot is built in mass-fraction coordinates):

$$X_{final} = -X_c\cdot\log_{10}(x_i/(1 - x_i));\ Y_{final} = -Y_c\cdot\log_{10}(x_i/(1 - x_i)) \quad (3)$$

The resulting plot is obtained from a triangular plot by stretching from its center point in 3 directions and hence called 3-way stretched. An example of this transformation is shown on Figure 9b. All available data for that system represent the solubility of the same component, Cefoxitin, which is component 3 in that mixture. There are two deficiencies in such a transformation. First, endpoints with zero content of one component cannot be represented by points (though they can be represented by asymptotic rays from the origin of the coordinates).

Second, if there are two components with small content, their ratio is not well represented (the translated points will lie close to the projection of the triangle vertices). A modification of this transformation is 1-way stretching where the same component is defined as minor for all data (even if its content is not the smallest) and same i is used for transformations of all data points (Eq. 3). In that case, only one side of the triangle is projected to infinite distance from the center. Solubility of the component declared minor in pure other components (endpoints of the solubility in the binary solvent) can be shown in this representation, but the second deficiency remains. Solubility of the Cefoxitin is represented in that way in Figure 9c.

The other proposed transformation for ternaries implies a definition of the solvent (component 3 in the example below). In that case, the X axis will represent $\log_{10}(x_1/x_2)$, and Y axis x_3 or $\log_{10}(x_3/(1 - x_3))$, depending on the type of equilibrium (Figures 10 and 11). The plot may contain a single isotherm or multiple isotherms distinguished by color, symbols, or connecting lines. Composition-stretched ternary diagrams (Figure 12) may reveal features not evident in the linear scale (Figure 2). Differences of the X coordinate between tied points in Figure 12 approximate the decimal logarithm of the distribution coefficient.

4. Conclusion

A way of representation of LLE and SLE data in binary and ternary systems has been developed that uniformly represents component ratios in the whole range of compositions. It is convenient for revealing trends, assessing data consistency or adequacy of models, and ultimately improving the quality of the published data. It will be implemented in the NIST ThermoData Engine[2] and is proposed for use when publishing or reviewing LLE and SLE data.

Supporting Information. Data and data sources used for illustration (Tables S1-S7); Mathematical transformations for ternary mixtures (a spreadsheet). This material is available free of charge via the Internet at http://pubs.acs.org.

REFERENCES

(1) Góral, M.; Shaw, D. G.; Mączyński, A.; Wiśniewska-Gocłowska, B.; Oracz, P. IUPAC-NIST Solubility Data Series. 96. Amines with Water. Part 3. Non-Aliphatic Amines. *J. Phys. Chem. Ref. Data*, **2012**, *41*, 043108.

(2) Diky, V.; Chirico, R. D.; Frenkel, M.; Bazyleva, A.; Magee, J. W.; Paulechka, E.; Kazakov, A. F.; Lemmon, E. W.; Muzny, C. D.; Smolyanitsky, A.; Townsend, S.; Kroenlein, K. NIST ThermoData Engine, NIST Standard Reference Database 103b-Pure Compounds, Binary Mixtures, and Chemical Reactions, version 10.1. Standard Reference Data Program, National Institute of Standards and Technology, Gaithersburg, MD, 2016.

(3) Alekseev, W. X. About solutions. *Ann. Phys. (Leipzig)*, **1886**, *28*, 305-338.

(4) Sidgwick, N. V.; Pickford, P.; Wilsdon, B. H. CXX. The Solubility of Aniline in Aqueous Solutions of its Hydrochloride. *J. Chem. Soc.*, **1911**, *99*, 1122-1132.

(5) Grozdanic, N.; Soldatovic, D.; Radovic, I.; Serbanovic, S.; Kijevcanin, M. Cloud Point Phenomena in the (Aniline or N,N-Dimethylaniline + Water) Solutions, and Cosolvent Effects of Liquid Poly(ethylene glycol) Addition: Experimental Measurements and Modeling. *J. Chem. Eng. Data*, **2015**, *60*, 493-498.

(6) Góral, M.; Shaw, D. G.; Mączyński, A.; Wiśniewska-Gocłowska, B.; Oracz, P. IUPAC-NIST Solubility Data Series. 101. Alcohols + Hydrocarbons + Water. Part 1. C_4–C_{10} Alcohols. *J. Phys. Chem. Ref. Data*, **2012**, *43*, 023101.

(7) Letcher, T. M.; Siswana, P. M. Liquid-liquid equilibria for mixtures of an alkanol + water + a methyl substituted benzene at 25 ºC. *Fluid Phase Equilib.*, **1992**, *74*, 203-217.

(8) Kim, Y.-K.; Ok, D.-S.; Park, D. W. Liquid-Liquid Equilibrium for the Quaternary System Water + Tetrahydrofuran + Toluene + 1-Butanol Mixture at 25 ºC and Atmospheric Pressure. *J. Chem. Eng. Data*, **2008**, *53*, 36-40.

(9) Possani, L. F. K.; Simões, R. L.; Staudt, P. B.; Soares, R. d. P. Mutual solubilities of hydrocarbon–water systems with F-SAC. *Fluid Phase Equilib.*, **2014**, *384*, 122-133.

(10) Hand, D. B. Dineric Distribution. *J. Phys. Chem.*, **1930**, *34*, 1961-2000.

(11) Othmer, D. F.; Tobias, P. E. Liquid-Liquid Extraction Data – Tie Line Correlation. *Ind. Eng. Chem.*, **1942**, *34*, 693-696.

(12) Calvar, N.; Gomez, E.; Gonzalez, B.; Dominguez, A. Experimental Determination, Correlation, and Prediction of Physical Properties of the Ternary Mixtures Ethanol + Water with 1-Octyl-3-methylimidazolium Chloride and 1-Ethyl-3-methylimidazolium Ethylsulfate. *J. Chem. Eng. Data*, **2007**, *52*, 2529-2535.

(13) Singh, T.; Kumar, A. Thermodynamics of dilute aqueous solutions of imidazolium based ionic liquids. *J. Chem. Thermodyn.*, **2011**, *43*, 958-965.

(14) Tariq, M.; Moscoso, F.; Deive, F. J.; Rodriguez, A.; Sanroman, M. A.; Esperanca, J. M. S. S.; Canongia Lopes, J. N.; Rebelo, L. P. N. Probing the self-aggregation of ionic liquids in aqueous solutions using density and speed of sound data. *J. Chem. Thermodyn.*, **2013**, *59*, 43-48.

(15) Kang, J. W.; Diky, V.; Frenkel, M. New modified UNIFAC parameters using critically evaluated phase equilibrium data. *Fluid Phase Equilib.*, **2015**, *388*, 128-141.

(16) Yuan, F.; Wang, Y.; Xiao, L.; Huang, Q.; Xu, J.; Jiang, C.; Hao, H. Solubility of cefoxitin acid in different solvent systems. *J. Chem. Thermodyn.*, **2016**, *103*, 125-133.

(17) Kiryukhin, A. M.; Lesteva, T. M.; Markuzin, N. P. Phase equilibriums in hydrocarbon-alcohol-water systems. I. Liquid-liquid equilibrium in systems with C_8 alcohols. *Prom-st Sint. Kauch.*, **1981**, 12-14.

(18) Kiryukhin, A. M.; Lesteva, T. M.; Markuzin, N. P. Phase equilibrium in hydrocarbon-alcohol-water systems. 3. Estimation of the separating action in systems containing C_8 alcohols. *Prom-st Sint. Kauch.*, **1983**, 3-6.

Figure captions

Figure 1. Mutual solubility data of aniline (1) + water (2) at p = 100 kPa or vapor saturation[3-5] in the linear scale (a), logarithmic scale (b), and the proposed composition-stretched scale (c). The data set highlighted by red color is from Grozdanic et al.[5]

Figure 2. LLE diagram for toluene + butan-1-ol + water at T = 298.15 K and at p =100 kPa built by TDE software[2] from selected literature sources[7-8]

Figure 3. Mutual solubility in the mixture 2-butoxyethan-1-ol (1) + water (2) at p =100 kPa or vapor saturation in the linear (a) and composition-stretched (b) representation. Data sources are given in the Supporting Information

Figure 4. Mutual solubility in the mixture propan-1-ol (1) + 1-butyl-3-methylimidazolium hexafluorophosphate (2) at p = 100 kPa or vapor saturation in the linear (a) and composition-stretched (b) representation. Data sources are given in the Supporting Information.

Figure 5. Speed of sound in water (1) + 1-methyl-3-octylimidazolium chloride (2) at p =100 kPa[12-14] in the linear-scale mole-fraction (a), mass-fraction (b), and composition-stretched (c) representation. Connecting lines form isotherms

Figure 6. LLE diagram for benzene (1) + water (2) at p =100 kPa or vapor saturation in the linear scale (a), logarithmic scale (b), and composition-stretched scale (c). Data sources are given in the Supporting Information. The model is NIST-modified UNIFAC[15] as implemented in ThermoData Engine[2]

Figure 7. LLE + SLE diagram for phenol (1) + water (2) at p =100 kPa in the linear scale (a) and composition-stretched scale (b). Data sources are given in the Supporting Information. The model is NIST-modified UNIFAC[15] as implemented in ThermoData Engine[2]

Figure 8. LLE data for aniline + water at p = 100 kPa or vapor saturation from Figure 1 represented in the composition-stretched scale. The uncertainties claimed by the authors (1 K and 0.0001 mole fraction) are displayed for the highlighted data set from Grozdanic et al.;[5] the other data are from Alekseev[3] (circles) and Sidgwick et al.[4] (triangles). Most of the claimed composition uncertainties are too small to protrude beyond the thickness of the temperature error bars

Figure 9. SLE diagram for methanol (1) + water (2) + Cefoxitin (3) at p = 100 kPa[16] in the triangle representation (a), 3-way composition-stretched representation according to Eq. 3, (b), and 1-way composition-stretched representation according to Eq. 3 (c). Minor component in (c) is Cefoxitin (i = 3 in Eq. 3 for all data). The transformations are given in the Supporting Information

Figure 10. LLE in the system benzene + ethanol + water at (298.15 ± 1) K and p = 100 kPa in the mole-fraction triangular representation (a) and solvent-explicit composition-stretched (x_{ethanol} vs $\log_{10}(x_{\mathrm{benzene}}/x_{\mathrm{water}})$ representation (b). The data and data sources are given in the Supporting Information. Data series are distinguished as follows: 1896 tay 0 (solid circles); 1899 lin 1 (dots); 1920 sid spu 0 (long dashes); 1921 orm cra 0 (hollow rhombs); 1926 bar 2 (hollow squares); 1931 was hni 0 (solid squares); 1936 var fen 0 (solid rhombs); 1942 ban hub 0 (hollow triangles); 1953 cha mou 0 (short dashes); 1961 mer nik 2 (hollow circles); 1990 let sew 0 (solid triangles)

Figure 11. LLE in the system water + hexane + 1-octanol at p =100 kPa or vapor saturation in the mole-fraction triangular built by TDE software[2] (a) and solvent-explicit composition-stretched ($\log_{10}(x_{\text{water}}/(1 - x_{\text{water}}))$ vs $\log_{10}(x_{\text{hexane}}/x_{\text{octanol}})$) (b) representations. The data are taken from 1981 Kiryukhin et al.[17] (circles) and 1983 Kiryukhin et al.[18] (triangles)

Figure 12. Solvent-explicit composition-stretched representation of tied LLE data for toluene + butan-1-ol + water at T = 298.15 K and p =100 kPa or vapor saturation. The data are Kim et al.[8]

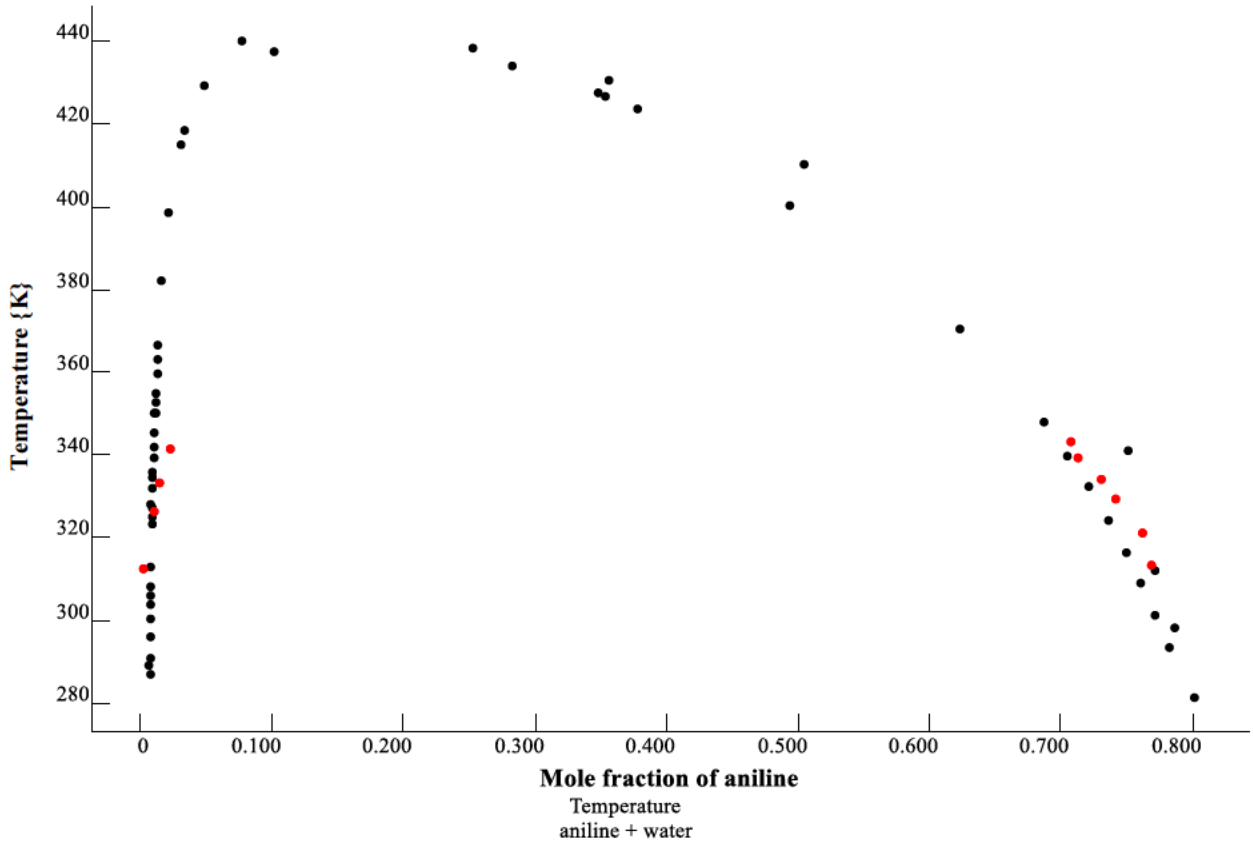
440
420
400
380
360
340
320
300
280
Temperature {K}
0
0.100
0.200
0.300
0.400
0.500
0.600
0.700
0.800
Mole fraction of aniline
Temperature
aniline + water

(a)

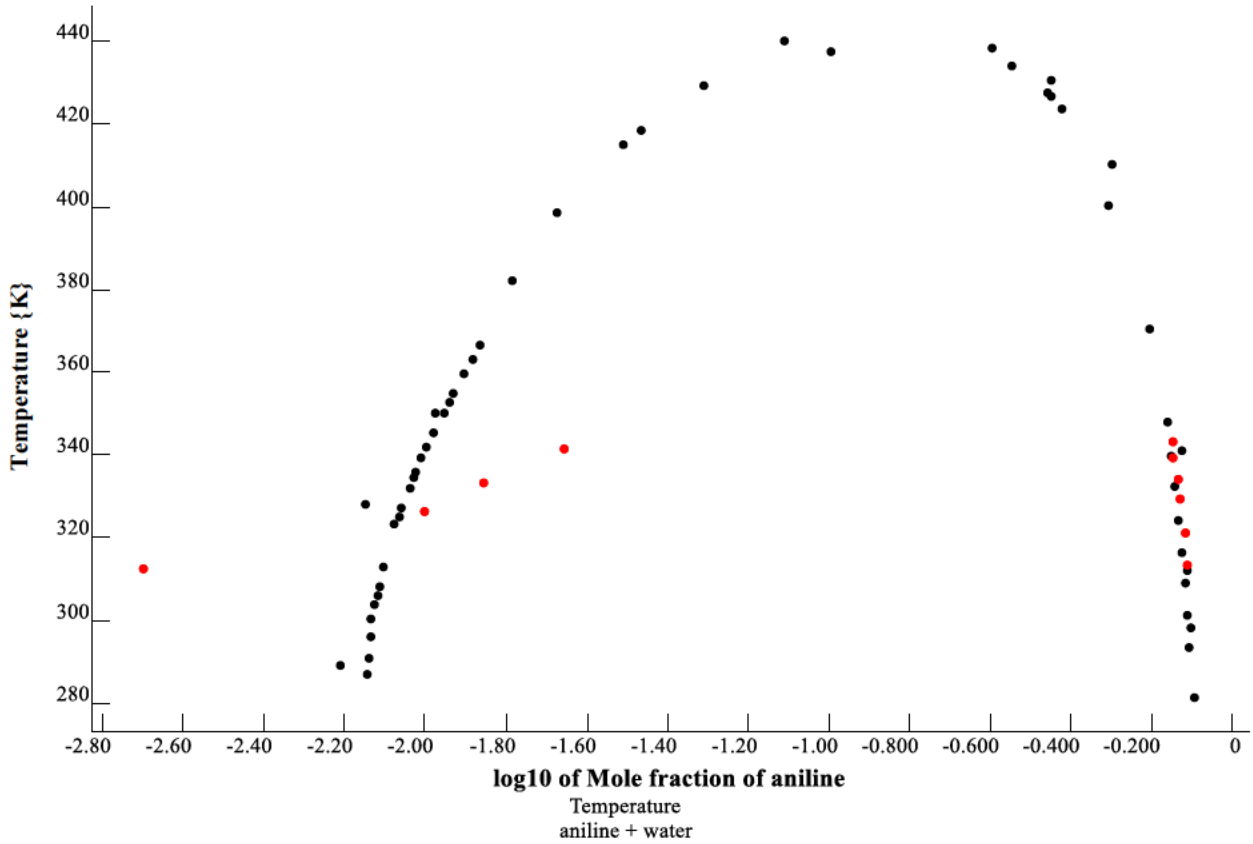
Temperature {K}
440
420
400
380
360
340
320
300
280
-2.80
-2.60
-2.40
-2.20
-2.00
-1.80
-1.60
-1.40
-1.20
-1.00
-0.800
-0.600
-0.400
-0.200
0
log10 of Mole fraction of aniline
Temperature
aniline + water

(b)

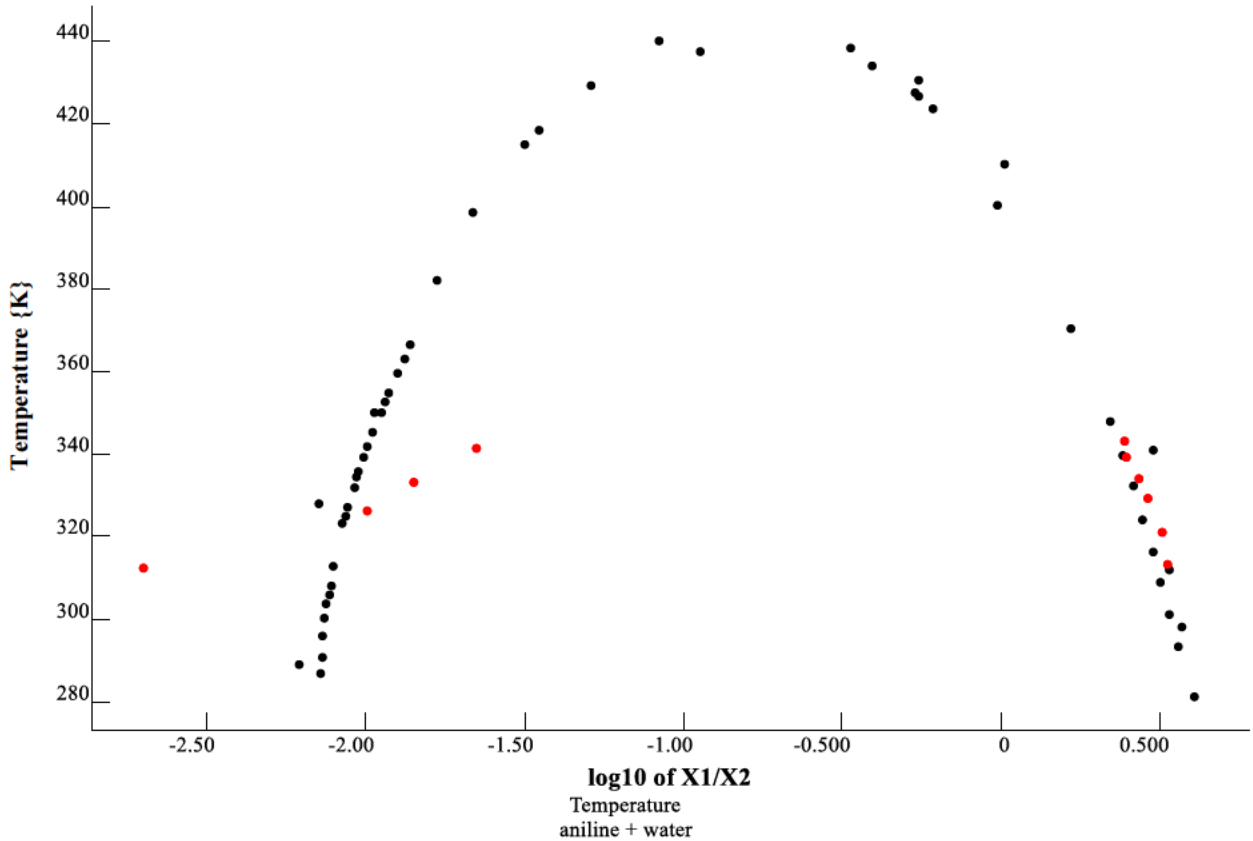

(c)

Figure 1. Mutual solubility data of aniline (1) + water (2) at p = 100 kPa or vapor saturation[3-5] in the linear scale (a), logarithmic scale (b), and the proposed composition-stretched scale (c). The data set highlighted by red color is from Grozdanic et al.[5]

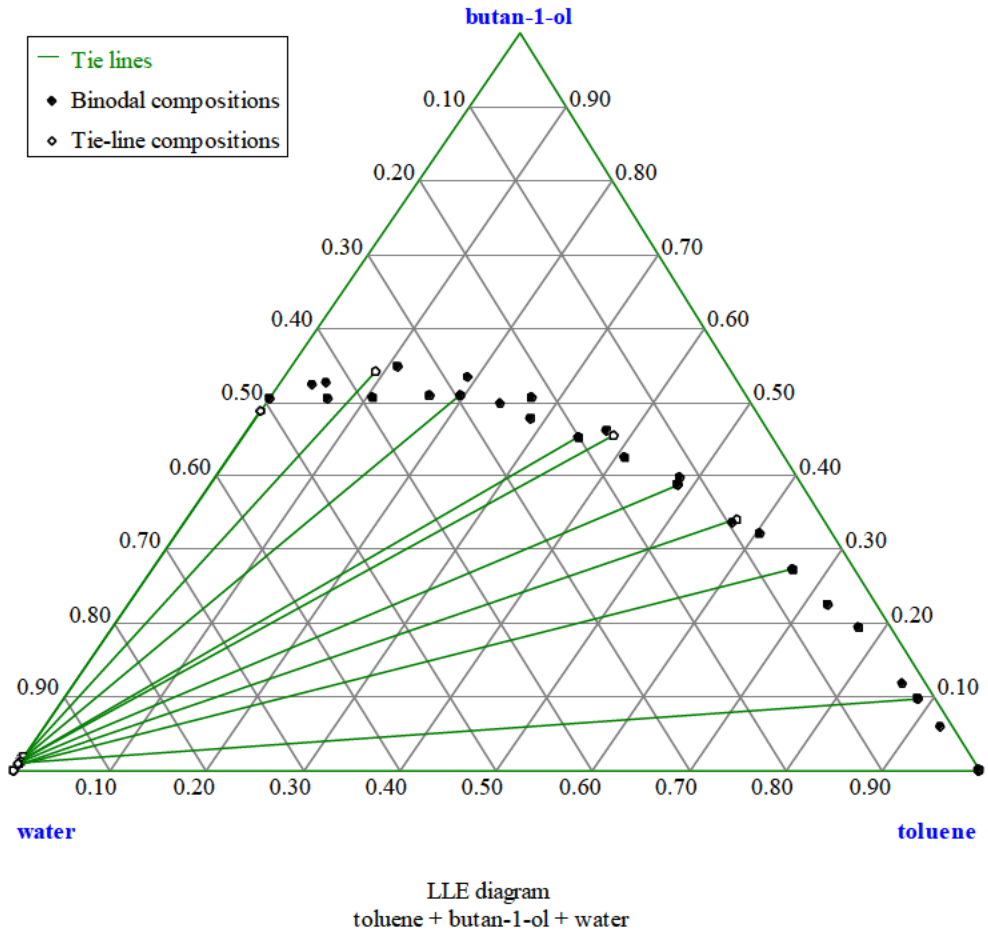

Figure 2. LLE diagram for toluene + butan-1-ol + water at T = 298.15 K and at p =100 kPa built by TDE software[2] from selected literature sources[7-8]

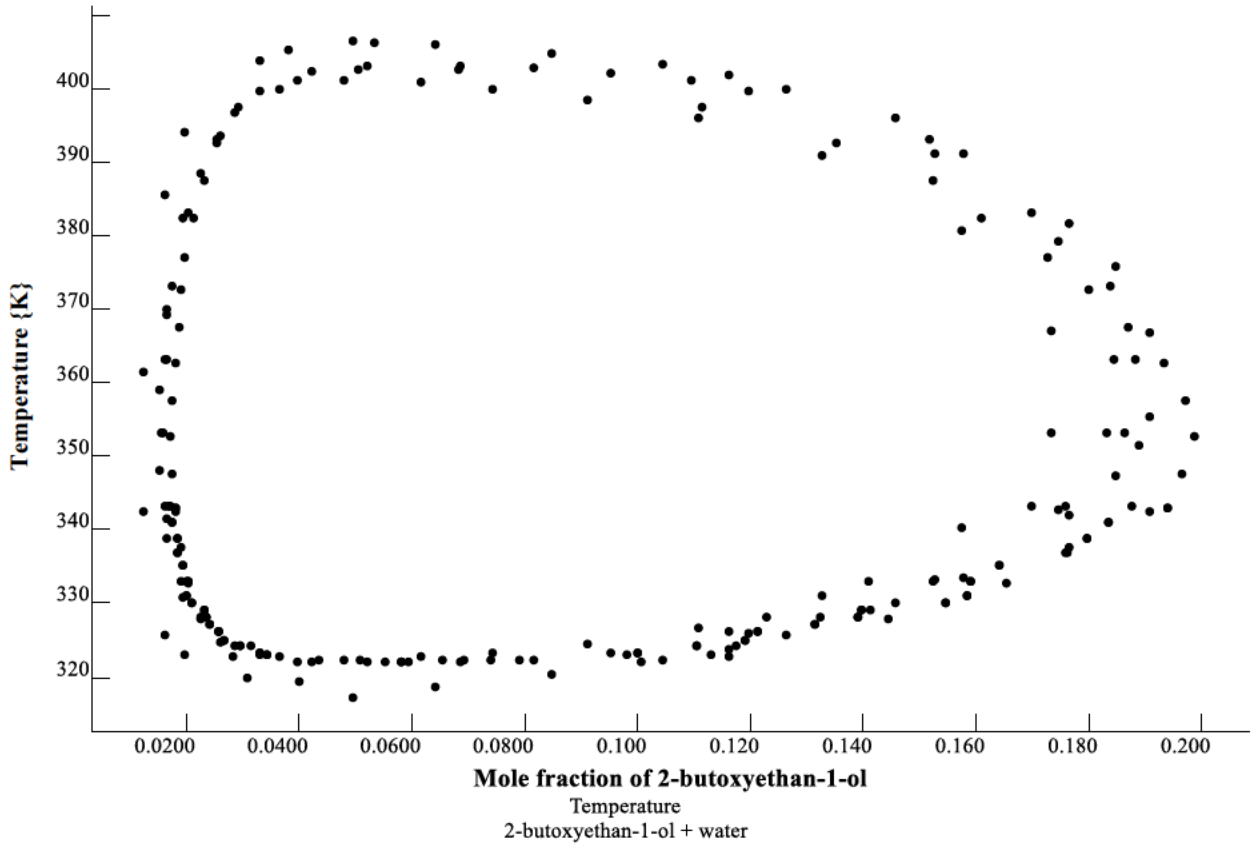
Temperature {K}
400
390
380
370
360
350
340
330
320
0.0200
0.0400
0.0600
0.0800
0.100
0.120
0.140
0.160
0.180
0.200
Mole fraction of 2-butoxyethan-1-ol
Temperature
2-butoxyethan-1-ol + water

(a)

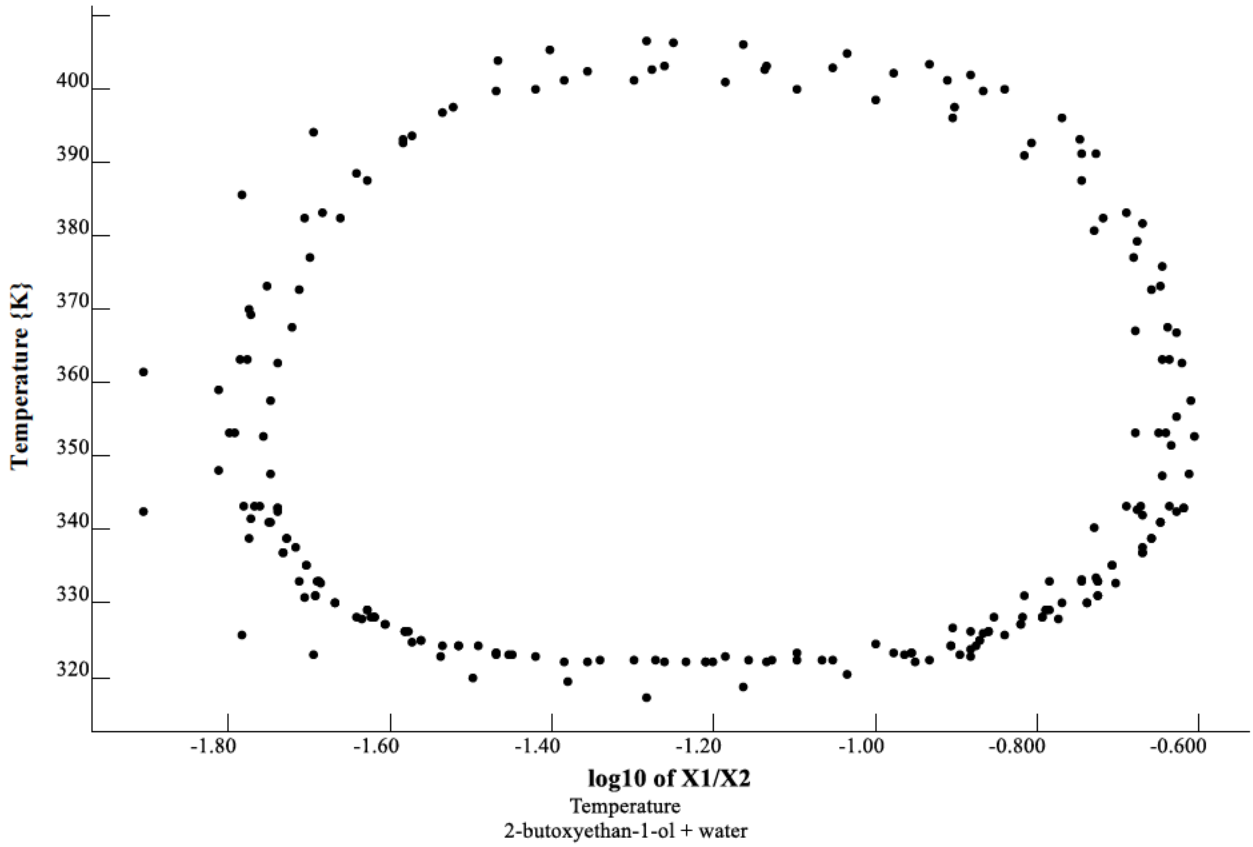

(b)

Figure 3. Mutual solubility in the mixture 2-butoxyethan-1-ol (1) + water (2) at p =100 kPa or vapor saturation in the linear (a) and composition-stretched (b) representation. Data sources are given in the Supporting Information

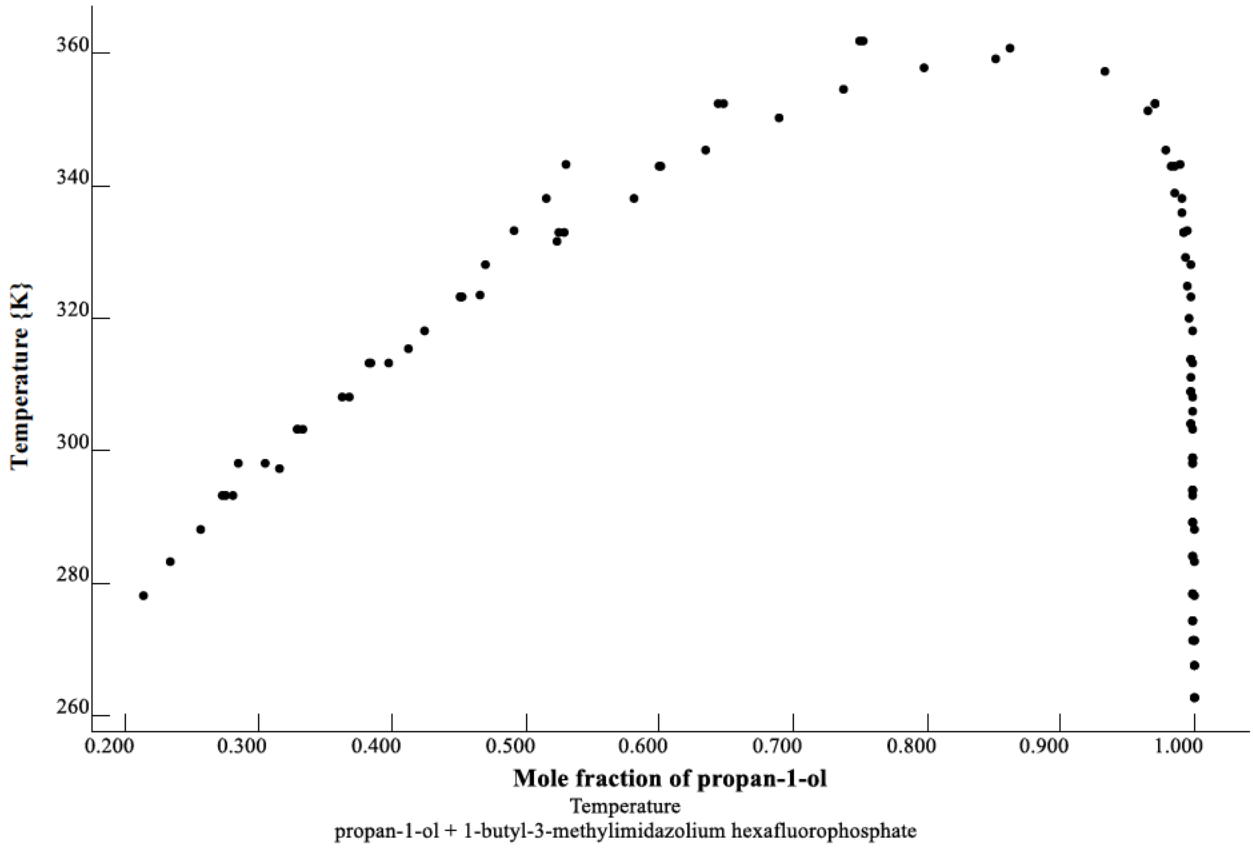
Temperature {K}
360
340
320
300
280
260
0.200
0.300
0.400
0.500
0.600
0.700
0.800
0.900
1.000
Mole fraction of propan-1-ol
Temperature
propan-1-ol + 1-butyl-3-methylimidazolium hexafluorophosphate

(a)

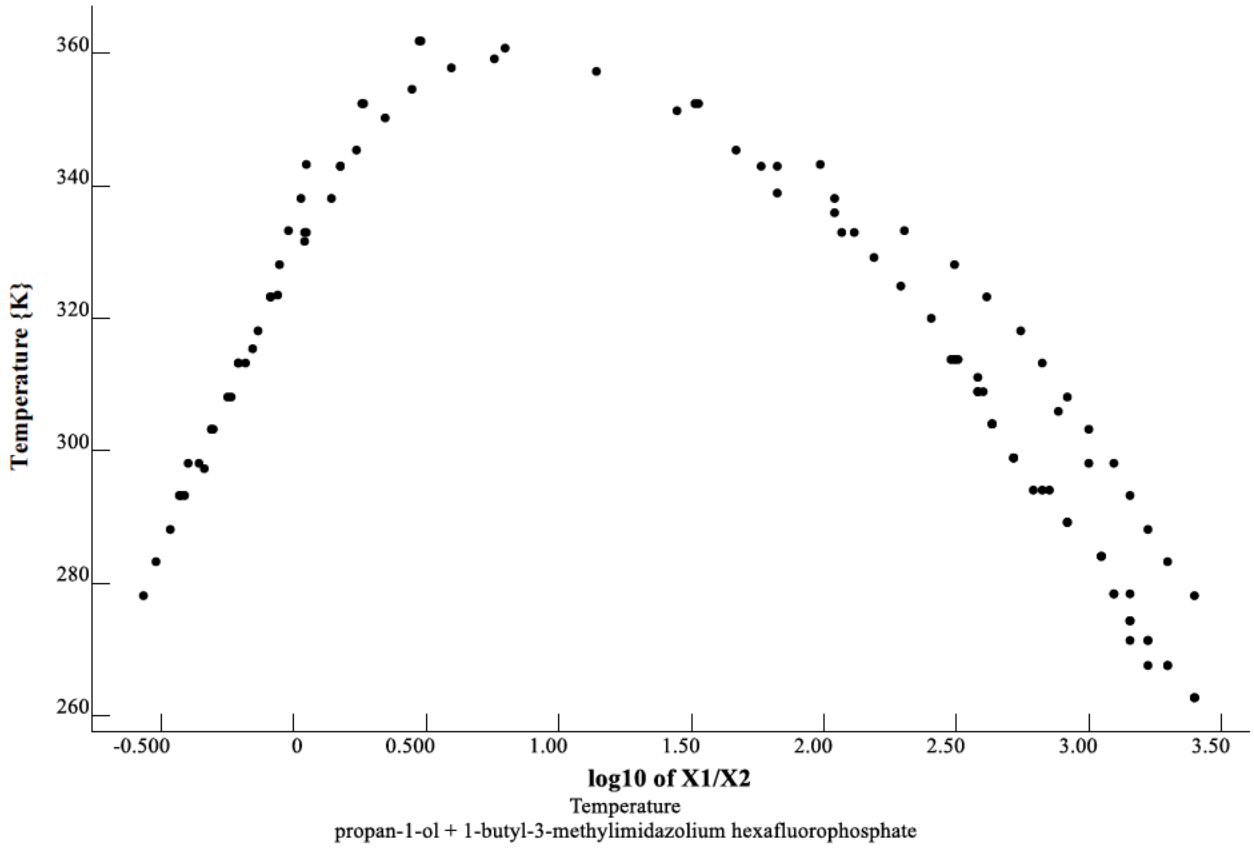

(b)

Figure 4. Mutual solubility in the mixture propan-1-ol (1) + 1-butyl-3-methylimidazolium hexafluorophosphate (2) at p = 100 kPa or vapor saturation in the linear (a) and composition-stretched (b) representation. Data sources are given in the Supporting Information.

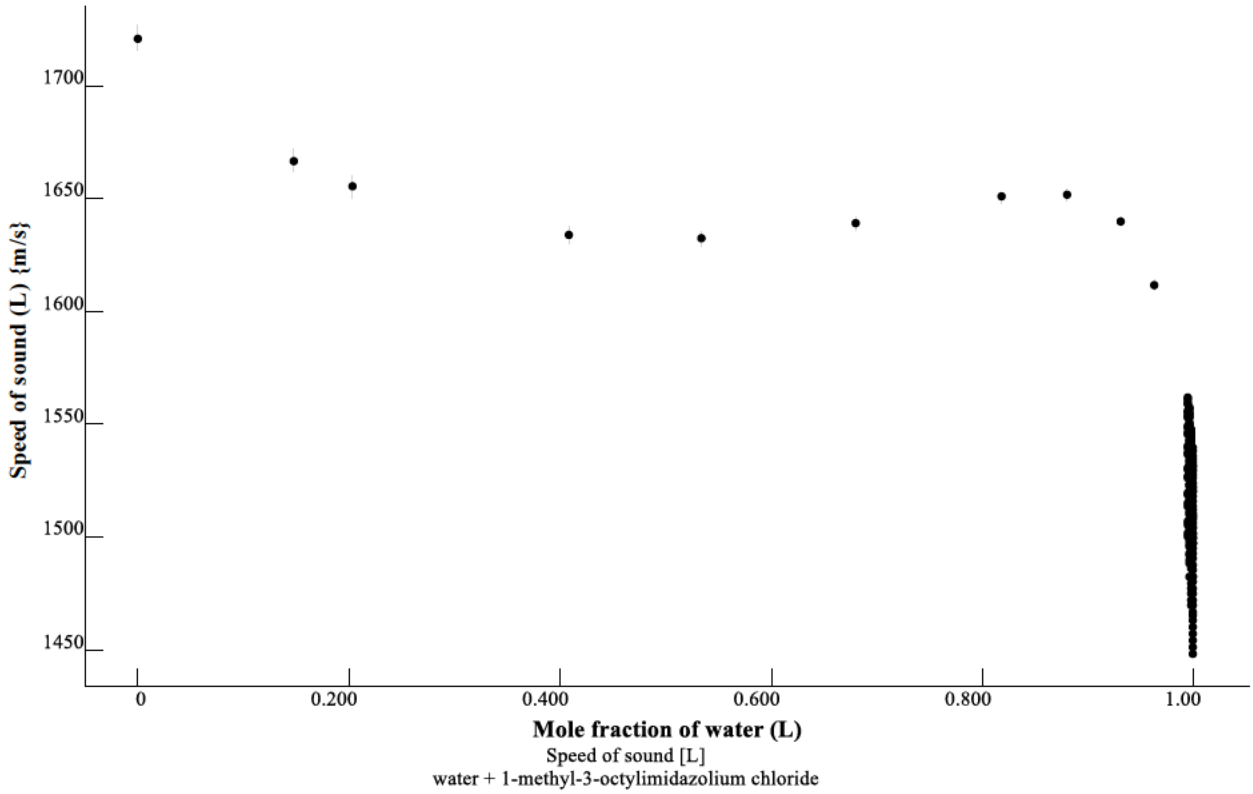
Speed of sound (L) {m/s}
1700
1650
1600
1550
1500
1450
0
0.200
0.400
0.600
0.800
1.00
Mole fraction of water (L)
Speed of sound [L]
water + 1-methyl-3-octylimidazolium chloride

(a)

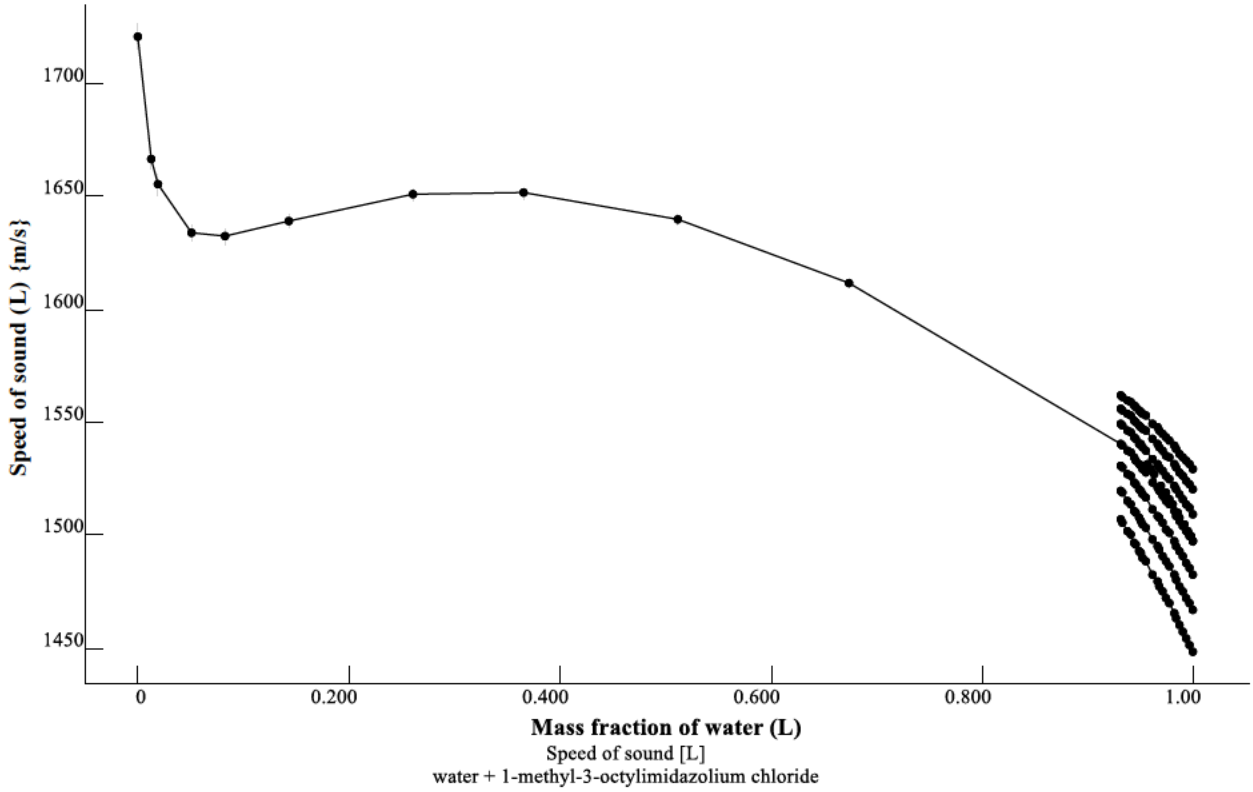
Speed of sound (L) {m/s}
1700
1650
1600
1550
1500
1450
0
0.200
0.400
0.600
0.800
1.00
Mass fraction of water (L)
Speed of sound [L]
water + 1-methyl-3-octylimidazolium chloride

(b)

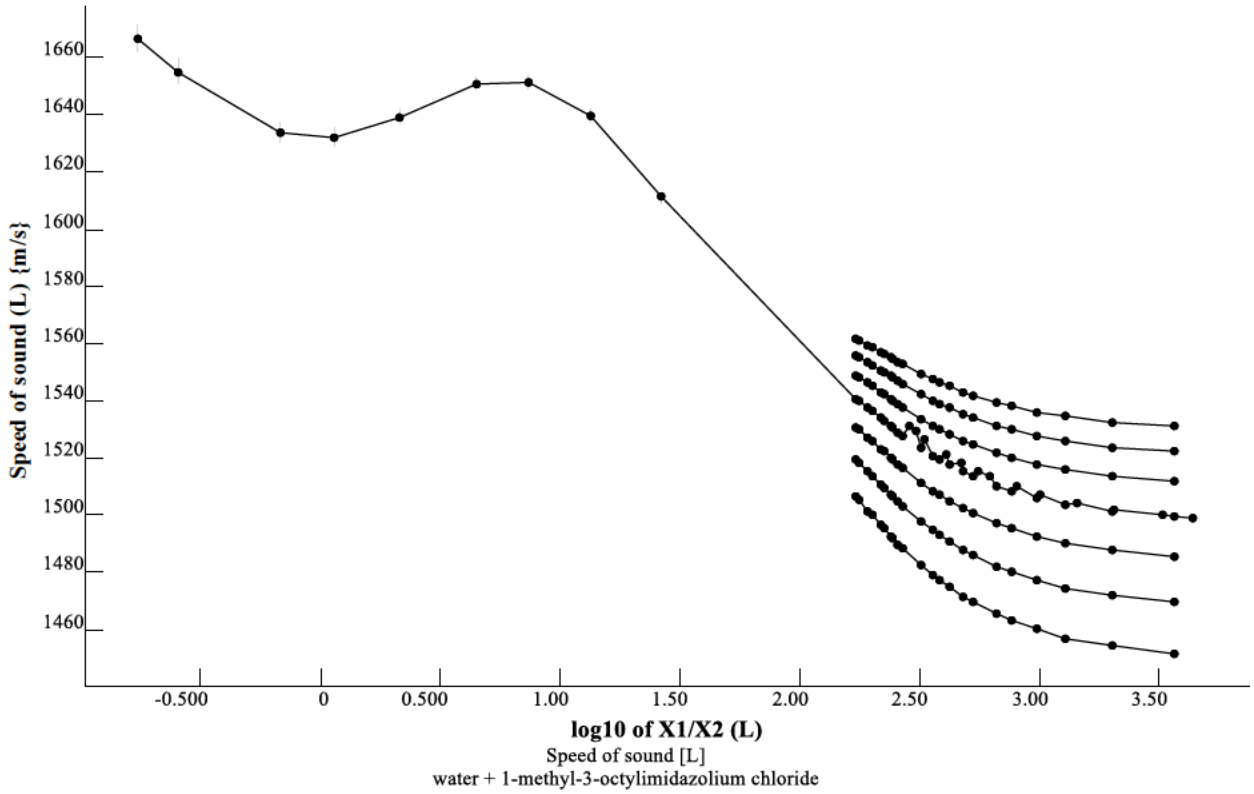

(c)

Figure 5. Speed of sound in water (1) + 1-methyl-3-octylimidazolium chloride (2) at p =100 kPa[12-14] in the linear-scale mole-fraction (a), mass-fraction (b), and composition-stretched (c) representation. Connecting lines form isotherms

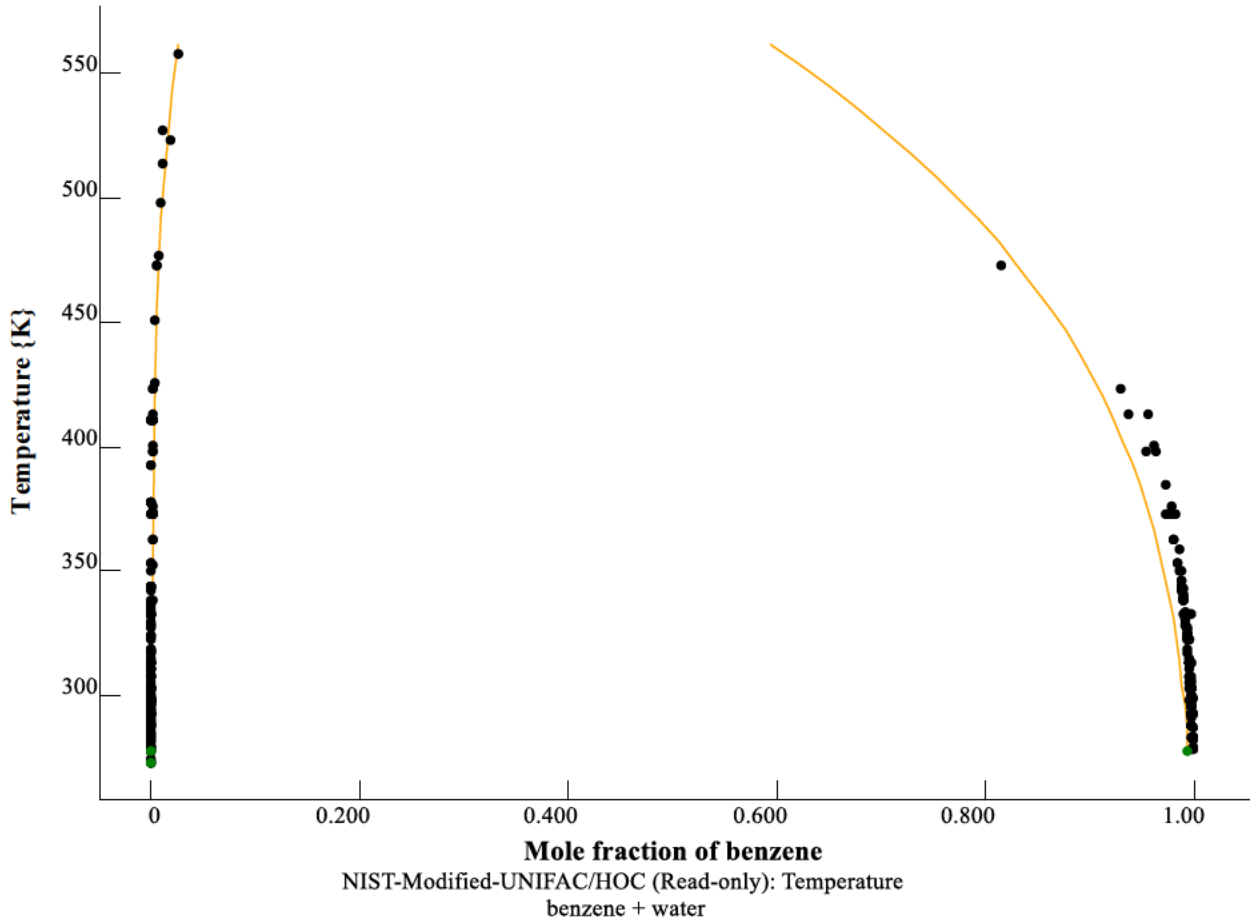
550
500
450
400
350
300
Temperature {K}
0
0.200
0.400
0.600
0.800
1.00
Mole fraction of benzene
NIST-Modified-UNIFAC/HOC (Read-only): Temperature
benzene + water

(a)

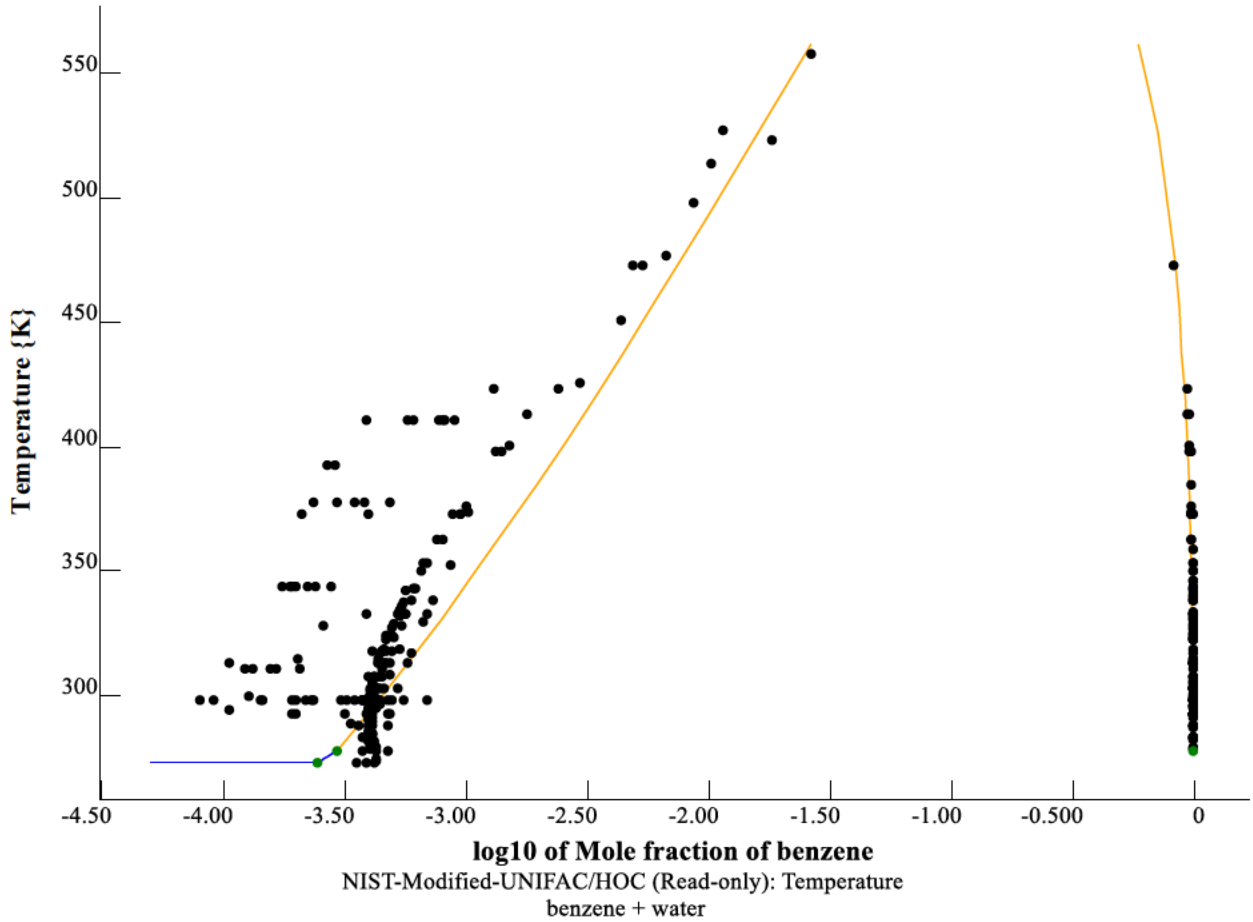
550
500
450
400
350
300
Temperature {K}
-4.50
-4.00
-3.50
-3.00
-2.50
-2.00
-1.50
-1.00
-0.500
0
log10 of Mole fraction of benzene
NIST-Modified-UNIFAC/HOC (Read-only): Temperature
benzene + water

(b)

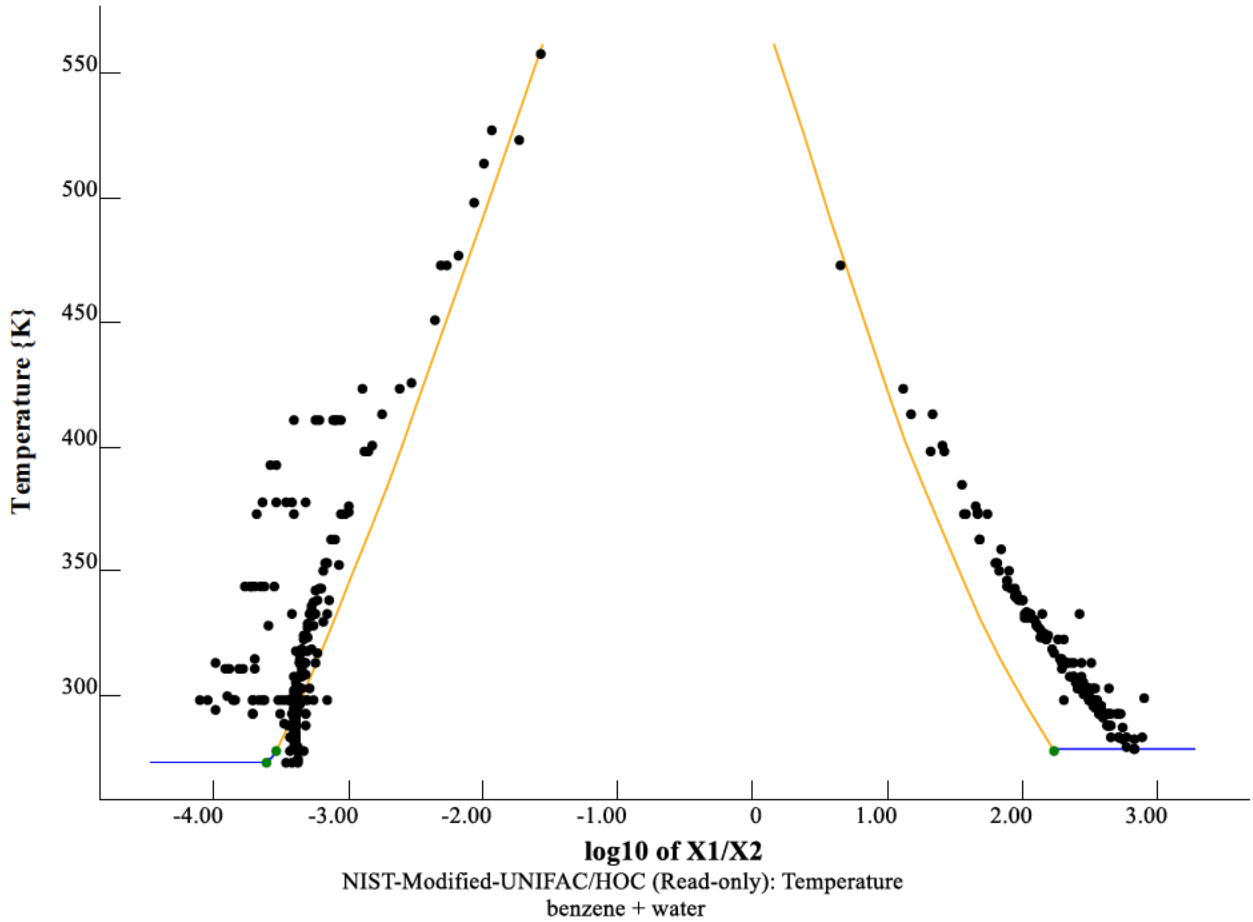

(c)

Figure 6. LLE diagram for benzene (1) + water (2) at p =100 kPa or vapor saturation in the linear scale (a), logarithmic scale (b), and composition-stretched scale (c). Data sources are given in the Supporting Information. The model is NIST-modified UNIFAC[15] as implemented in ThermoData Engine[2]

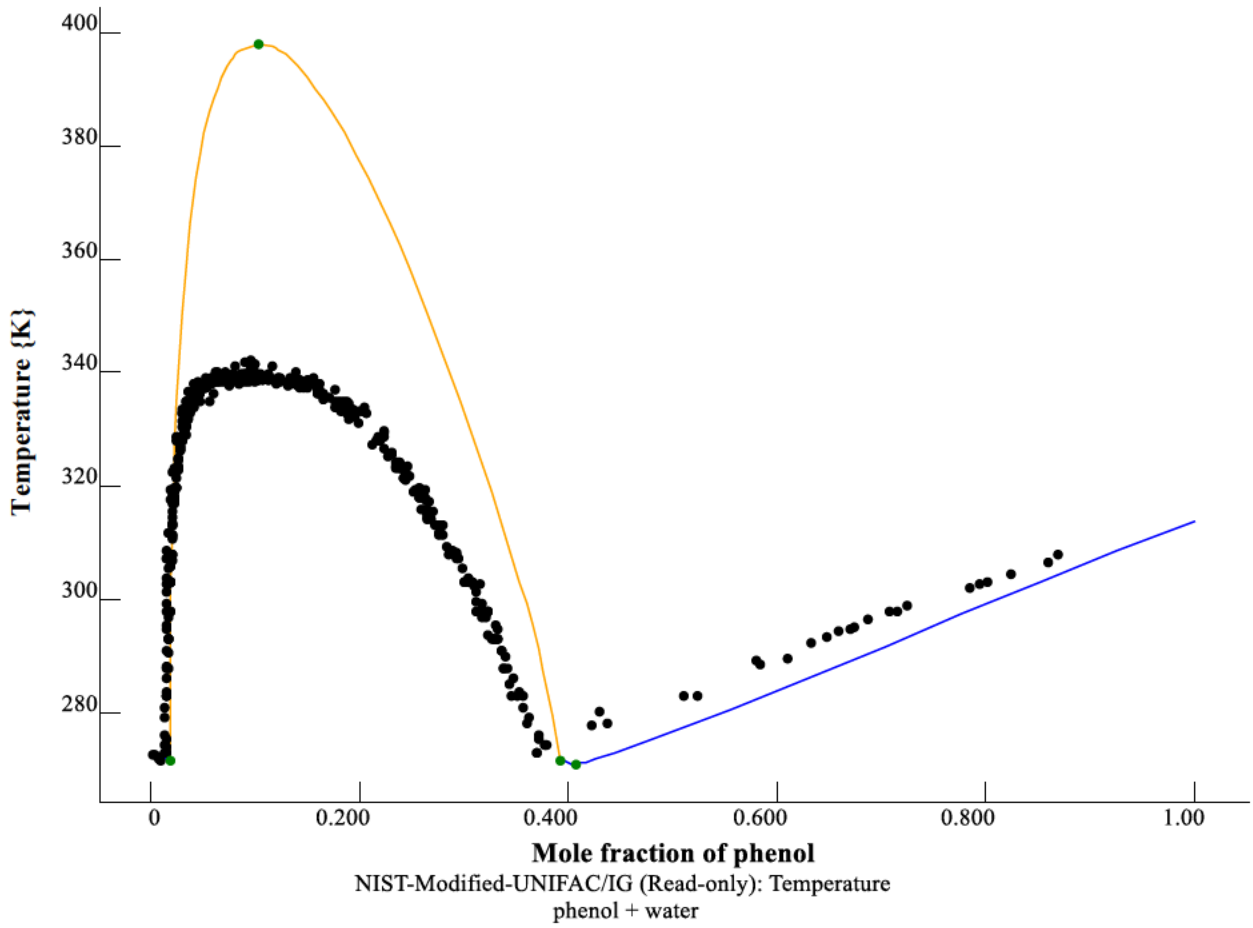
400
380
360
340
320
300
280
Temperature {K}
0
0.200
0.400
0.600
0.800
1.00
Mole fraction of phenol
NIST-Modified-UNIFAC/IG (Read-only): Temperature
phenol + water

(a)

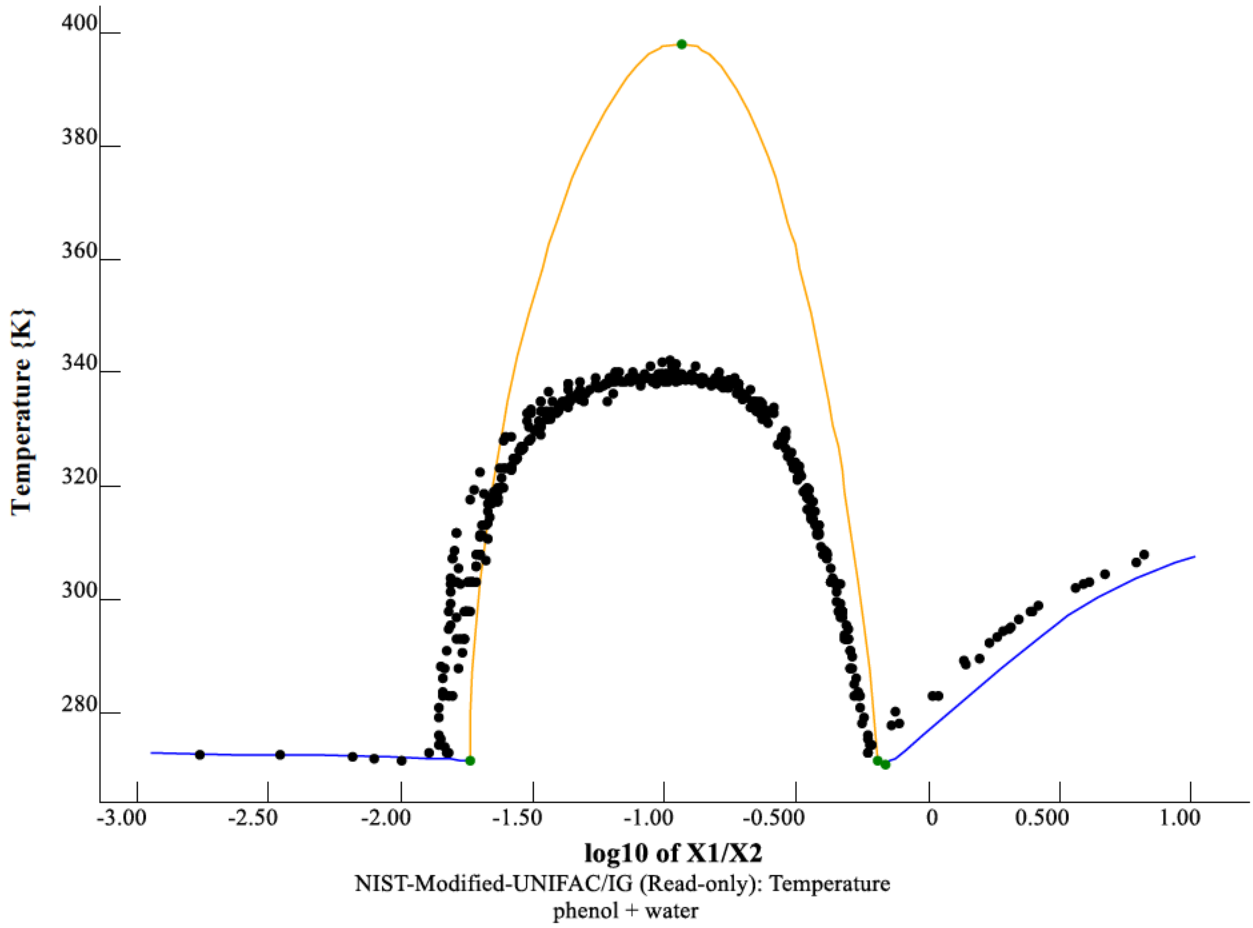

(b)

Figure 7. LLE + SLE diagram for phenol (1) + water (2) at p =100 kPa in the linear scale (a) and composition-stretched scale (b). Data sources are given in the Supporting Information. The model is NIST-modified UNIFAC[15] as implemented in ThermoData Engine[2]

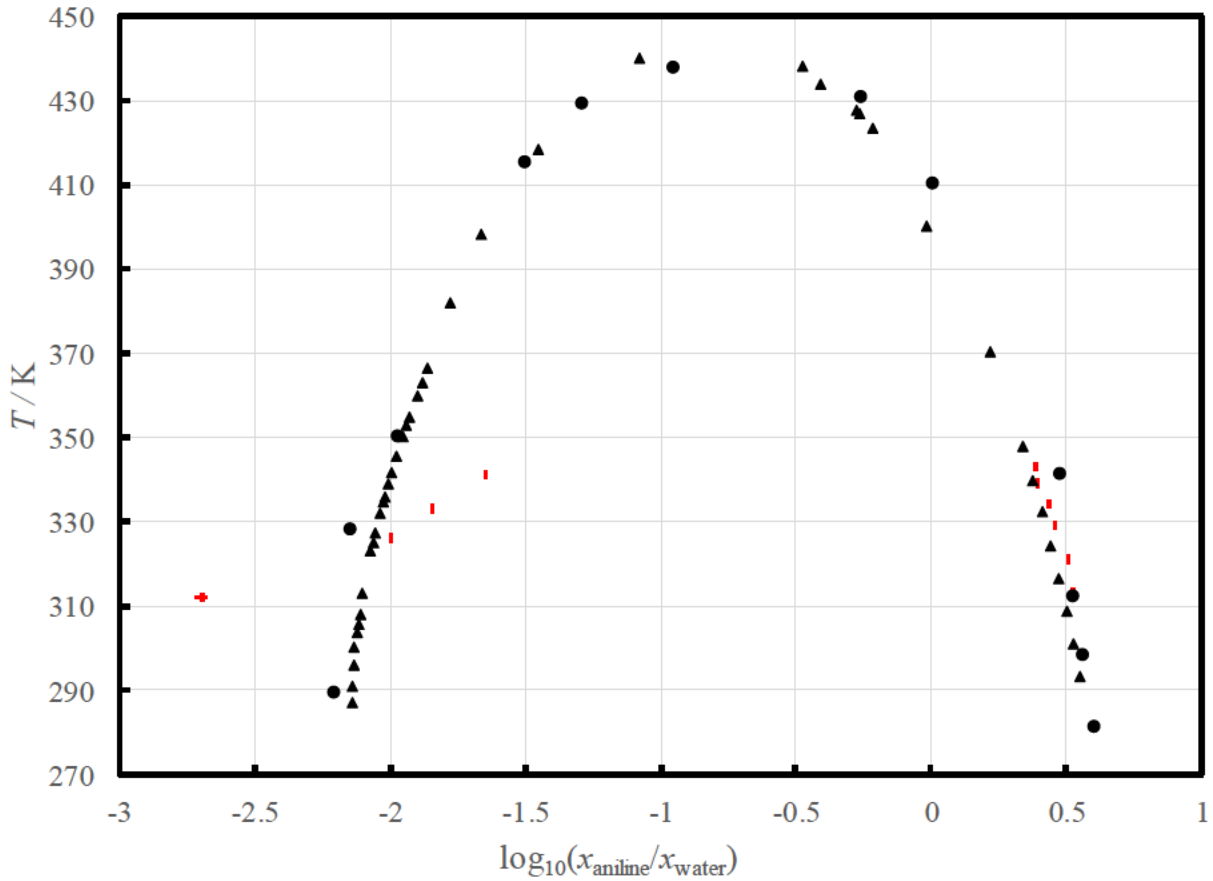

Figure 8. LLE data for aniline + water at p = 100 kPa or vapor saturation from Figure 1 represented in the composition-stretched scale. The uncertainties claimed by the authors (1 K and 0.0001 mole fraction) are displayed for the highlighted data set from Grozdanic et al.;[5] the other data are from Alekseev[3] (circles) and Sidgwick et al.[4] (triangles). Most of the claimed composition uncertainties are too small to protrude beyond the thickness of the temperature error bars

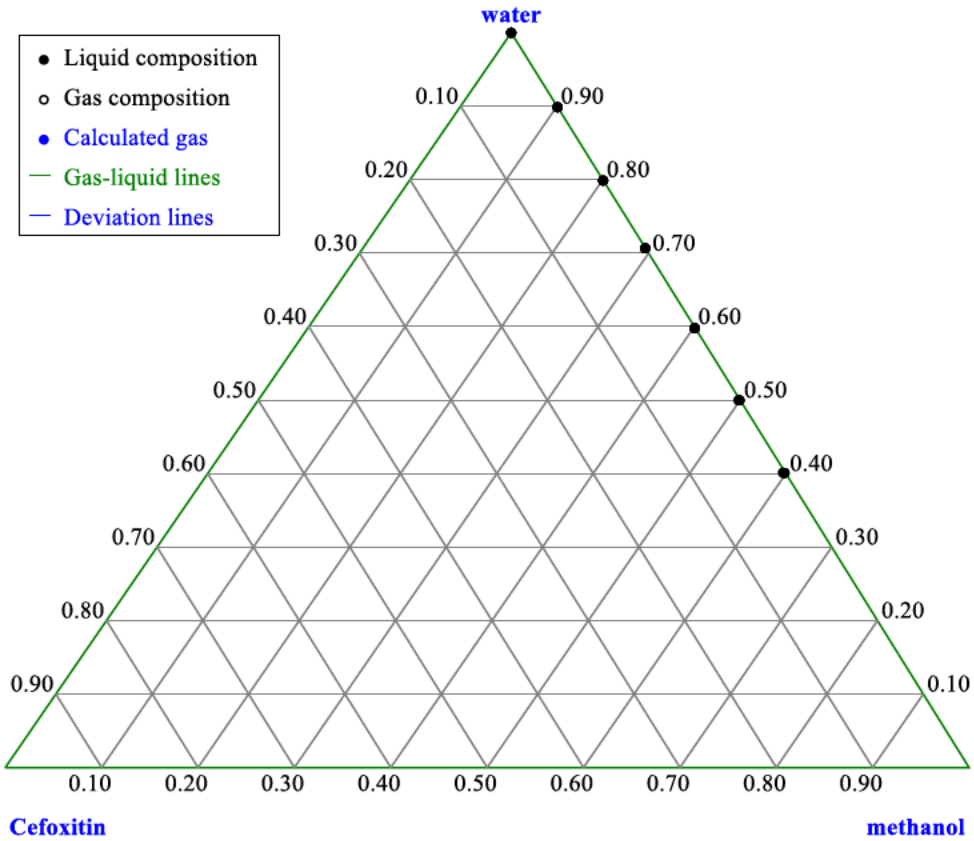

SLE diagram
methanol + water + Cefoxitin

(a)

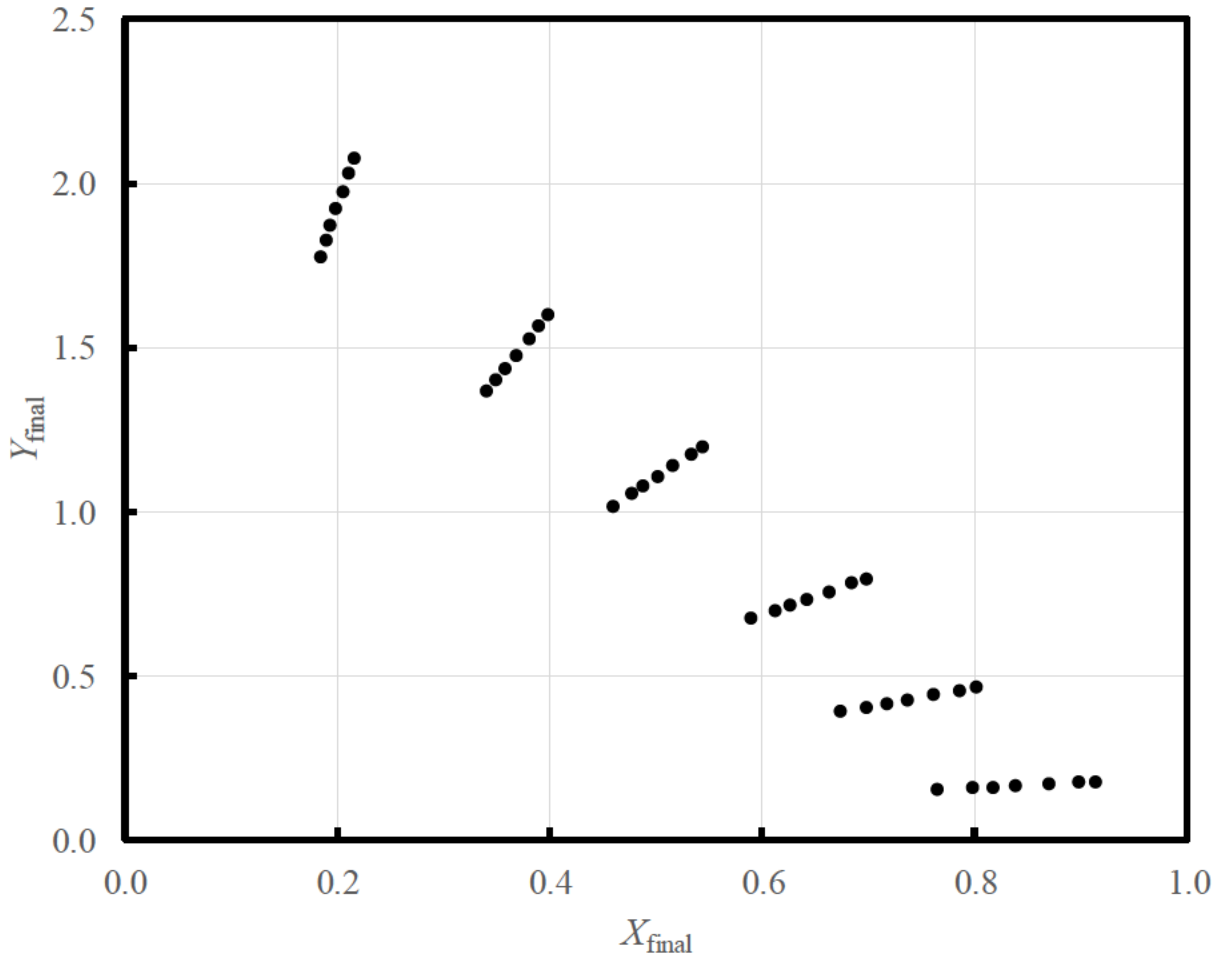

(b)

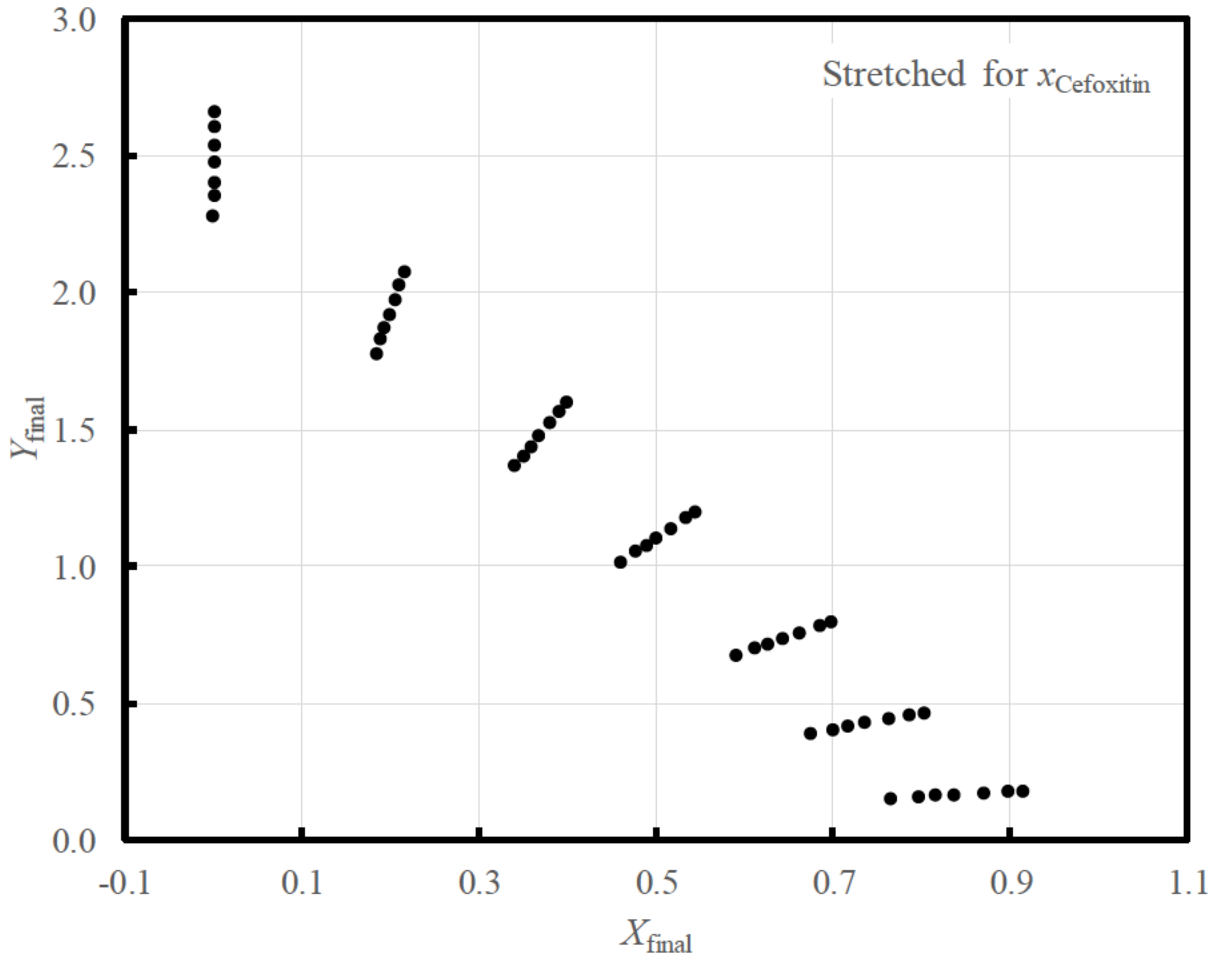

(c)

Figure 9. SLE diagram for methanol (1) + water (2) + Cefoxitin (3) at p = 100 kPa[16] in the triangle representation (a), 3-way composition-stretched representation according to Eq. 3, (b), and 1-way composition-stretched representation according to Eq. 3 (c). Minor component in (c) is Cefoxitin (i = 3 in Eq. 3 for all data). The transformations are given in the Supporting Information

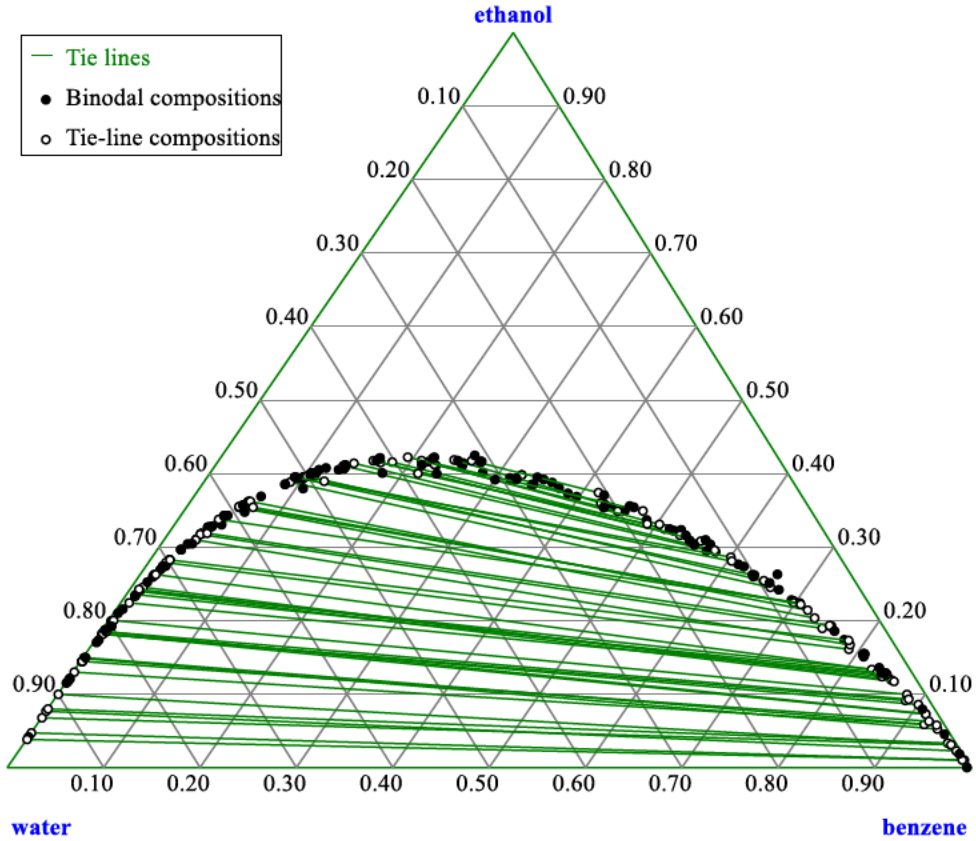

LLE diagram
benzene + ethanol + water

(a)

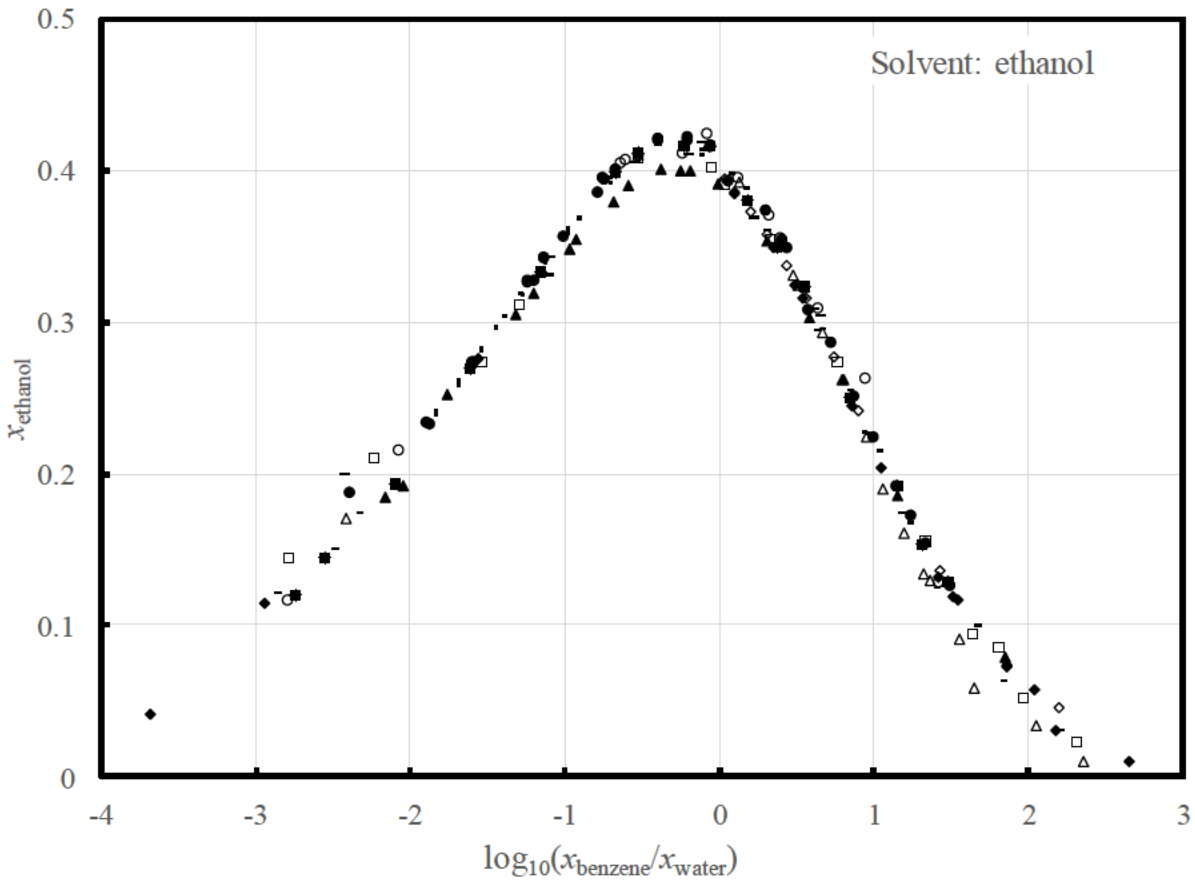

(b)

Figure 10. LLE in the system benzene + ethanol + water at (298.15 ± 1) K and p = 100 kPa in the mole-fraction triangular representation (a) and solvent-explicit composition-stretched ($x_{ethanol}$ vs $\log_{10}(x_{benzene}/x_{water})$ representation (b). The data and data sources are given in the Supporting Information. Data series are distinguished as follows: 1896 tay 0 (solid circles); 1899 lin 1 (dots); 1920 sid spu 0 (long dashes); 1921 orm cra 0 (hollow rhombs); 1926 bar 2 (hollow squares); 1931 was hni 0 (solid squares); 1936 var fen 0 (solid rhombs); 1942 ban hub 0 (hollow triangles); 1953 cha mou 0 (short dashes); 1961 mer nik 2 (hollow circles); 1990 let sew 0 (solid triangles)

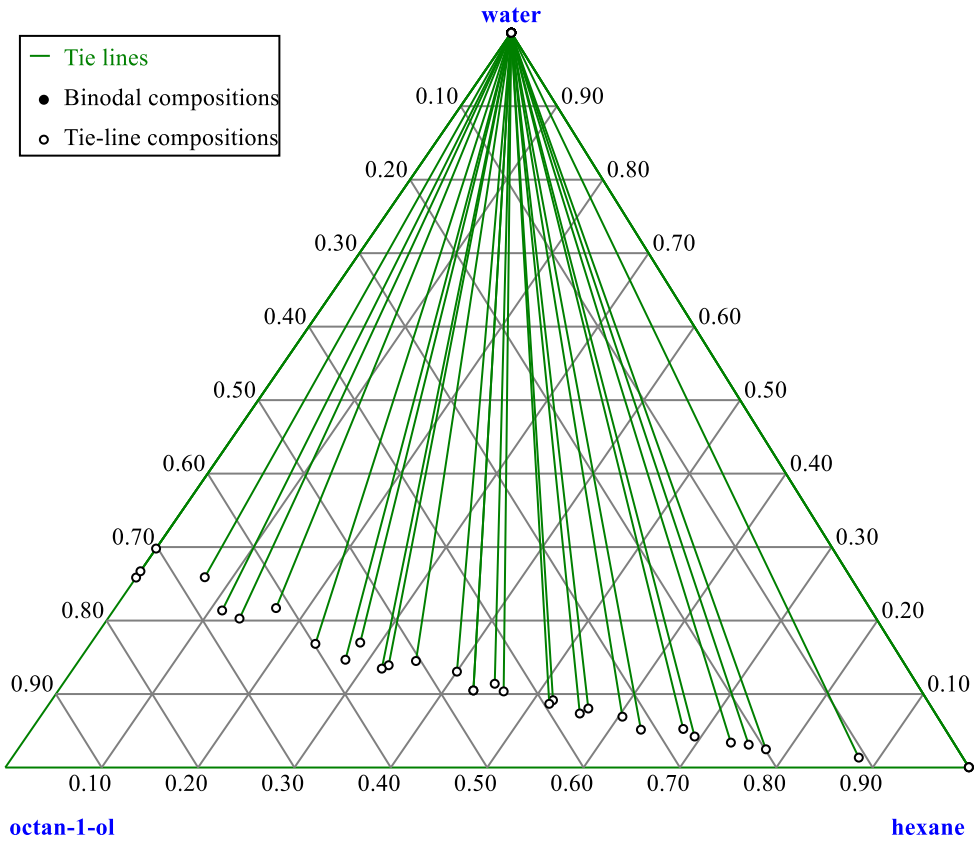

LLE diagram
hexane + water + octan-1-ol

(a)

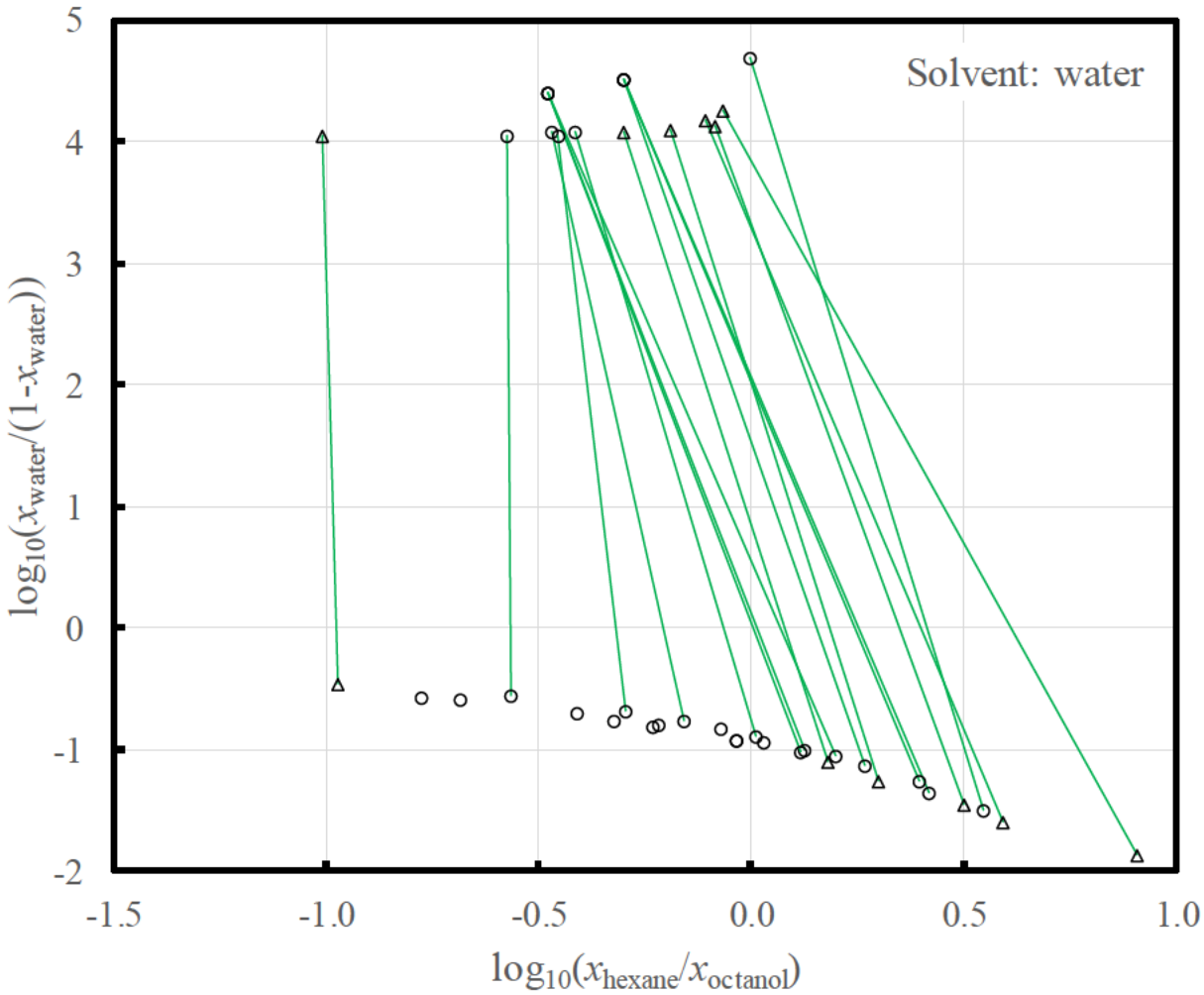

(b)

Figure 11. LLE in the system water + hexane + 1-octanol at p =100 kPa or vapor saturation in the mole-fraction triangular built by TDE software[2] (a) and solvent-explicit composition-stretched ($\log_{10}(x_{water}/(1 - x_{water}))$ vs $\log_{10}(x_{hexane}/x_{octanol})$) (b) representations. The data are taken from 1981 Kiryukhin et al.[17] (circles) and 1983 Kiryukhin et al.[18] (triangles)

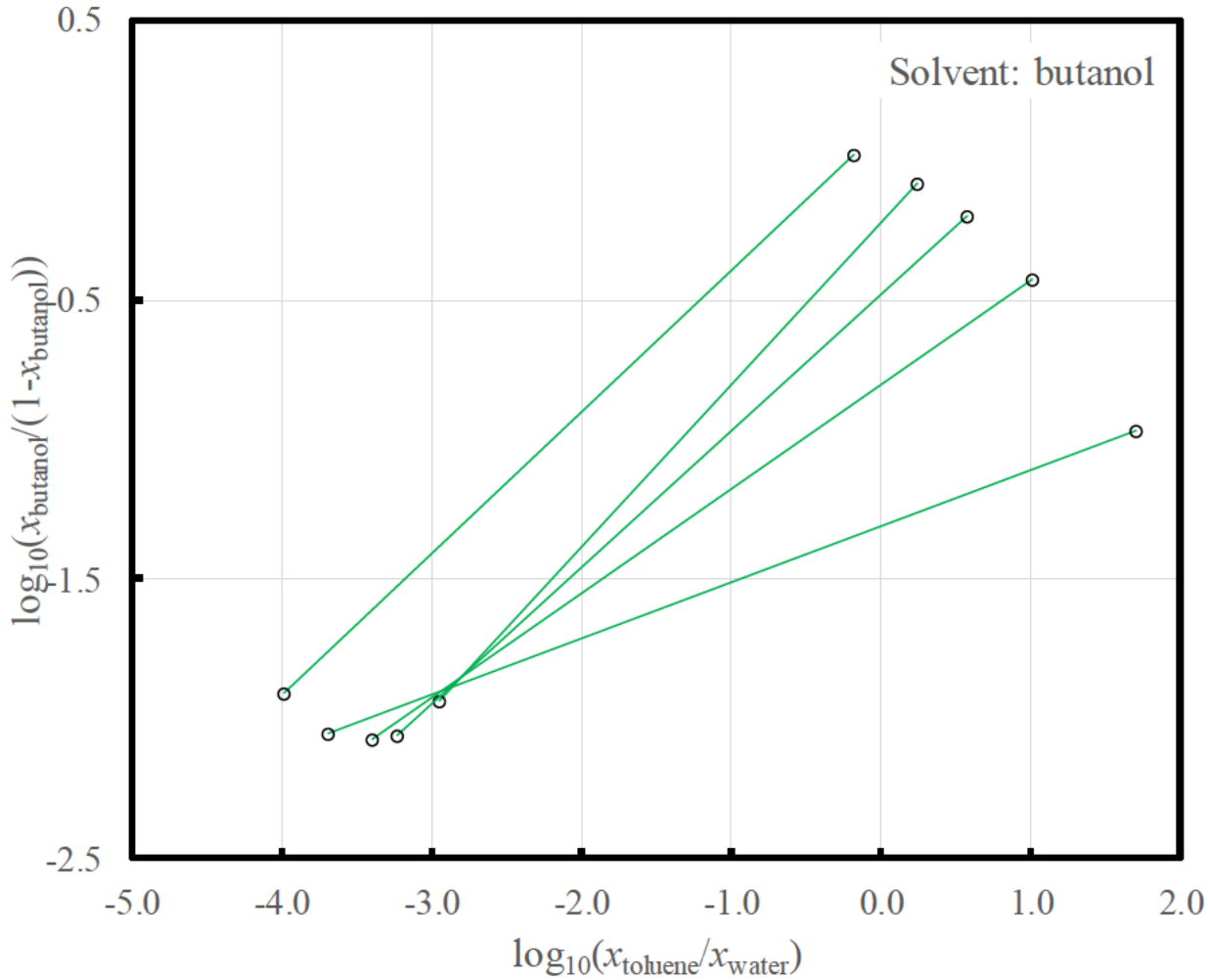

Figure 12. Solvent-explicit composition-stretched representation of tied LLE data for toluene + butan-1-ol + water at T = 298.15 K and p =100 kPa or vapor saturation. The data are Kim et al.[8]

TOC Graphics

Traditional linear scale

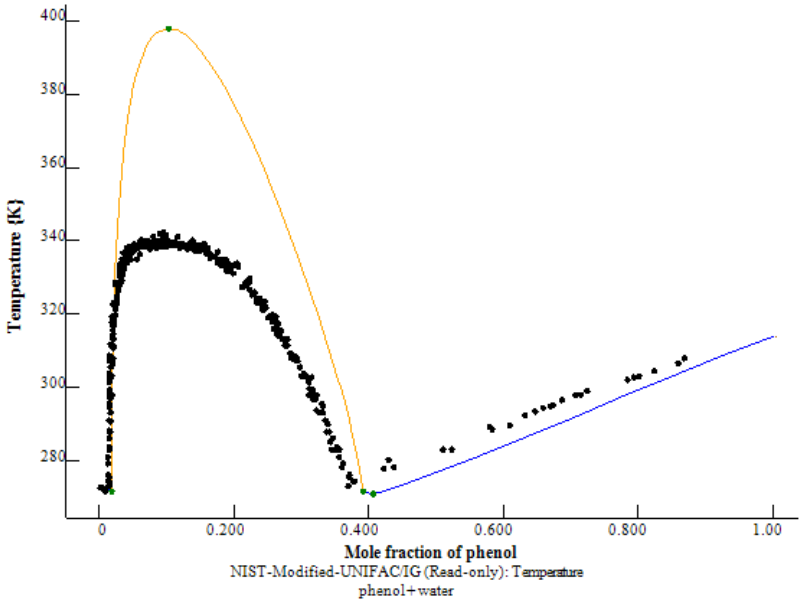

Composition-stretched scale